Nonlinear Transport

in Hamiltonian Pump-Ratchet Hybrids

Nicolás Medina Sánchez

Universidad Nacional de Colombia
Facultad de Ciencias, Departamento de Física
Bogotá, Colombia
Year 2019

Nonlinear Transport
in Hamiltonian Pump-Ratchet Hybrids

Nicolás Medina Sánchez

This thesis is presented for the degree of:
Ms.C. in Physics

Director:
Ph.D. Thomas Dittrich

Investigation Topic:
Nonlinear Dynamics - Chaos Theory
Investigation Group:
Chaos & Complexity

Universidad Nacional de Colombia
Facultad de ciencias, Departamento de Física
Bogotá, Colombia
Year 2019

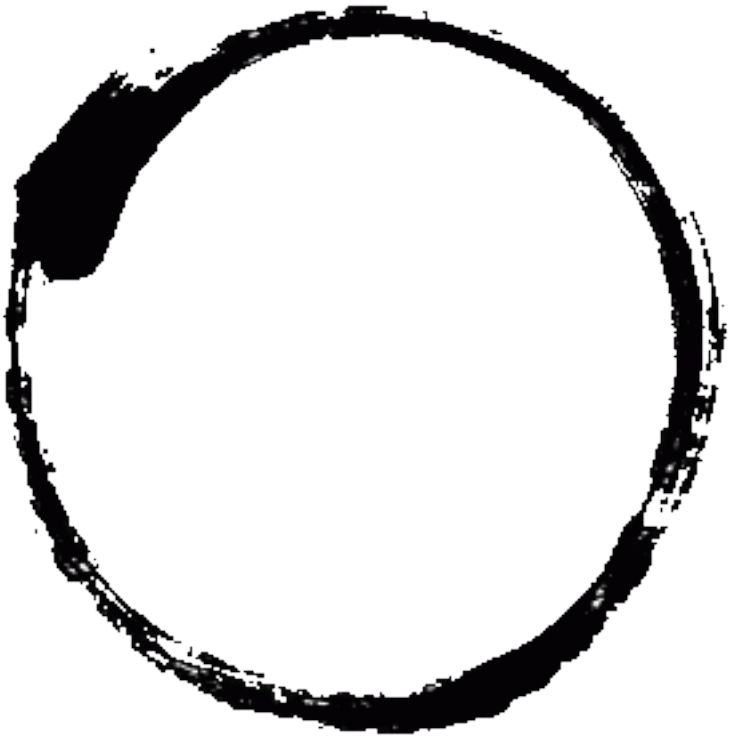

When the hubless wheel turns,
Even the master would be at a loss what to do,
It turns above heaven and beneath earth,
South, north, east, and west.

Mumonkan, kōan VIII

Acknowledgements

To my family, that support me along all this work, believing in what I could not even believe.

This project was partially sponsored by the Universidad Nacional de Colombia through the HERMES project No. 41466.

Abstract

The pumps and ratchets are benchmark prototypes of systems that generate directed transport. In this work we introduce a possible hybrid between these systems, using a model in a Hamiltonian fashion, that combines a spatially periodic static potential with a local driving, with different possibilities of space inversion and time reversal symmetry breaking. In this way, we found manifestations of irregular scattering that leads to net current generation for three types of general models of punchets found, in terms of the way they break the symmetries. Also, is showed how this currents depends on the symmetry manipulation parameters of the model. Further, an approximation to the quantum version of punchets shows discrete energy shifts induced by the periodic time-dependence of the driving as long as asymptotic Bloch states scatters.

Keywords: Pump, Ratchet, Directed Transport .

Index

1. Introduction

Nonlinear transport mechanisms are present in a wide range of natural phenomena affine to diverse natural sciences. In physics [23, 19], chemistry [16], biology [7], and beyond [27], systems where a privileged direction in physical space exists, in terms of motion of information, are of high interest. In particular, those systems where the cause of this isotropy breaking is a consequence of strong nonlinear dynamics, when that means that the asymmetry origin is a nonlinear response to some stimulus applied to the system.

The technical advantages at engineering level that this kind of mechanisms could achieve, have been exploited in recent years through the design of a wide family of dispositives capable of generate this type of asymmetrical behaviour. From thermal and electric rectifiers, to switches and transistors of different kinds, coming from different physical mechanisms: electric fields [10], magnetic fields [29], physical barriers [21] and also pumped liquid in channels [18].

In the literature we found typically two main theoretical structures that can develop this type of directed behaviour; namely, the **Ratchets** and **Pumps**, which are symmetry-breaking devices that can be defined in a recursive way: pumps are just ratchets restricted to some physical domain, and ratchets are just chains of pumps. This will be discussed broadly in the following chapter. In physical sciences, this kind of systems typically are studied in the framework of solid-state physics, using crystalline materials subjected to a time-dependent force. Examples of this are metallic and semiconductor surfaces under laser pumping [13, 12] and polymers illuminated by a CW laser [20].

The previous examples, moreover, not only shows phenomenological manifestations of the induced directed transport mechanisms, but also of devices in which the time-dependent force acts only in a compact region in space, that is, only in some cells of the crystalline structure. This kind of systems, where the anisotropy is induced by a mixed work between local driving and crystalline structures, is what we called **Punchets**, due to the hybrid form that it has between ratchets and pumps.

The theoretical interest in this kind of hybrid mechanisms is that they resemble, in essence, a scattering scenario with a time-dependent target and asymptotical non-free states, but the ones of the crystalline system. This manifests questions at classical and quantum level that can not be properly solved using the theoretical tools existing for the study of ratchets and

pumps by itself. The purpose of this thesis is to introduce, for a specific model of punchet, a classical and quantum approximation to the directed transport phenomena that arouse in this systems.

This kind of mechanisms manifests also strong possibilities of current control, due to the existence of a broad family of parameters that regulate the symmetry-breaking through the scattering. Depending on the way we can break the necessary symmetries, is possible to typify a family of essential 3 types of punchets. The first type consists of a scattering region that breaks the time-reversal symmetry while the crystalline asymptotic structure breaks the spatial inversion symmetry. A second possible model is basically a type of pump, where both time and space inversion symmetries are broken by the scattering potential. A final model couples both symmetries in the scattering region using a travelling wave, resembling the so called peristaltic ratchets[28], but whose action is bounded to the scattering region.

The first chapter of this thesis, **Pumps and Ratchets** is an introduction to the underlying mechanisms of breaking symmetries that generates directed transport in the scenarios of pumps and ratchets.

After this, in **Classical Scenario** we define the Punchet and describe a 1D hamiltonian model for one example of them. This description is make in terms of the directed transport analysis, firstly constructing the stroboscopic maps for the dynamics, and looking for strong oscillations and fractality in reaction functions, typifying in this way possible irregular (chaotic) dynamics for the model. After this, we show the single contributions (trajectory at trajectory) to the transport phenomena and finally computing net currents for the 3 mentioned types of punchets, analyzing the dependence of the direction of the currents of the parameters in the model.

In **Quantum Scenario** we analyze the quantum version of the introduced punchet model. First, we look for the band structure of the crystalline asymptotic structures in order to characterize the asymptotic states. Then, we show a phase-space representation of the scattering in terms of the Husimi-Kano Q function, useful for graphic analysis of the wave-packet behaviour. Finally, we show that scattering process indeed generate energy shifts to the incident wave-packet, as it is predicted by the Floquet analysis of the system.

2. Pumps & Ratchets

In this chapter, we introduce the basic elements of the theory of directed transport in the two frameworks that will be central to the development of this work. Each theoretical scenario has a family of features that identifies them and whose mixed manipulation will be the main object of the analysis held in this thesis.

Nevertheless, punchets carry characteristics by itself that arose only in the hybrid scenario. This will be the topic of the following chapters.

2.1. Pumping Theory

The core idea behind pumping is the generation of DC currents between asymptotic physical systems with the same bias [3]. The device in charge of the occurrence of this phenomena is the *pump*, that can be understood as a localized system between the asymptotic scenarios (also reservoirs), that generates a net current of some physical degree of freedom (mass, charge, angular momentum, etc.), from one system (A) to the other (B).

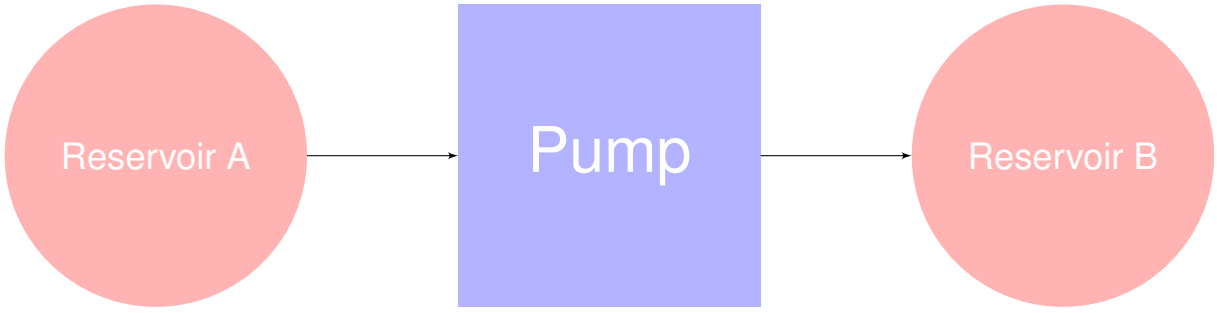

The idea behind this kind of systems arose in the context of current generation in material media, without energy dissipation. In this context, a periodic (AC) perturbation on the system conduces a DC current, that is not consequence of taking the system far from its equilibrium state, which is the underlying current generation mechanism when dissipation is present [1]. This feature, makes possible the generation of currents even in the adiabatic regime.
Examples of this kind of systems were firstly semiconductor quantum dots between electrodes at the same bias [3]. This kind of pumps take advantage of the Coulomb blockade, that is basically the dominance of the electronic repulsion in small systems under low voltages. Coupling (weakly) two quantum dots at the Coulomb blockade regime, configure a pump in the sense

that directed currents, from one quantum dot to the other, emerge when we apply sinusoidal voltages to each quantum dot at constant phase difference [22]. Pumps can be constructed also from a single quantum dot [25] where there is an adiabatic variation of a couple of parameters that modifies the quantum mechanical properties of the system. The generated current is proportional to the frequency of this adiabatic control. An important characteristic of this mechanisms is the possibility of reverse the current direction only reversing the phase between the two control parameters.

This initial proposals states barely that it is necessary for the current generation the existence of two out-of-phase time-dependent control parameters. However, recent experimental achievements show that single-parameter quantum pumps are possible [8]. The idea behind this is that the phase difference between the parameters are essential for the two-parameters pumping, because of the phase shift that this generates in the parameter space. However, this phase shift is characteristic in other type of physical scenarios, for example, in the presence of a magnetic potential. Therefore, it is not necessary two parameters to the phase shift generation. This current control can be reversed, inverting the phase shift generation, that in the case of the magnetic field consists only in its direction inversion.

The relevance of complex dynamics in this kind of systems was initially discussed in terms of the failure, for chaotic scenarios, of the Linear Response Theory analysis of the causal relations between external driving and generated phenomena. There, the manifestation of chaotic structures in phase-space will lead to diffusion blocking, due to Kolmogorov-Arnold-Moser structures [4]. Moreover, in the specific case of closed systems, we have that the directed transport behaviour is indeed a manifestation of a mixed phase-space structure [24].

2.2. Ratchet Theory

Ratchets and pumps are closely related structures. Some authors, indeed, do not make a well-defined discrimination between them, assuring that ratchets are just pumps but with a necessarily nonlinear pumping mechanism [5]. In the framework of this thesis, the distinction between them relies basically in the spatial domain of the driving on the physical system. While in pumping we need a localized notion of system that will be understood as the pump, in ratchet theory this localization does not hold anymore. Then, the ratchets are also directed transport mechanisms but the driving force is manifest in all the system.

However, the ratchet concept has its origin in the motion in biological motors. These motors are characterized by conformational changes that strongly restrict the possible motion at each step. Then, the main characteristic of a ratchet is the bias at each step of the motion between the possibilities for the next step. This is modelled by a potential energy surface that is periodic

and asymmetric (e.g. saw tooth potential) [17]. At each period of the potential, the minimum confines particles that does not have the sufficient energy to surpass the period barrier. So this is not sufficient for the directed transport expected. In order to complete this we have to introduce an energy source that helps the bounded particles to get out from the minimum. This can be done via a thermal bath, for open systems, or using some kind of the driving, when, in both cases, the essential source of transport is the breaking of the time reversal symmetry. This occurs natural in open systems, but in closed ones, this means a special structure of the driving.

There are different types of ratchets, starting from the pulsating ones, that consists of ratchets that oscillates between two potential states, as a consequence of the time dependence. The tilting ratchet, in other hand, preserves its shape in time, but has an oscillating force that is applied across all the system. An essential difference in the physical mechanisms that underlies both types, is that the tilting produces net currents even if the oscillation frequency is infinitely slow (adiabatic phenomena). An interesting characteristic is that neither of this types can generate currents if the oscillation frequency is faster than the typical timescales of the system. A third type is the peristaltic ratchet, that consists of a simultaneous translation in space and time of the potential [28].

A single period of a ratchet can be considered as a pump. Therefore, an analogue description for ratchets is to see it as a periodic chain of coupled pumps. This integrates very nice with the image presented in the previous section about the pump mechanism. Here, we have a collection of pumps in which, for each pump, the reservoirs are just the income and outcome of other pumps.

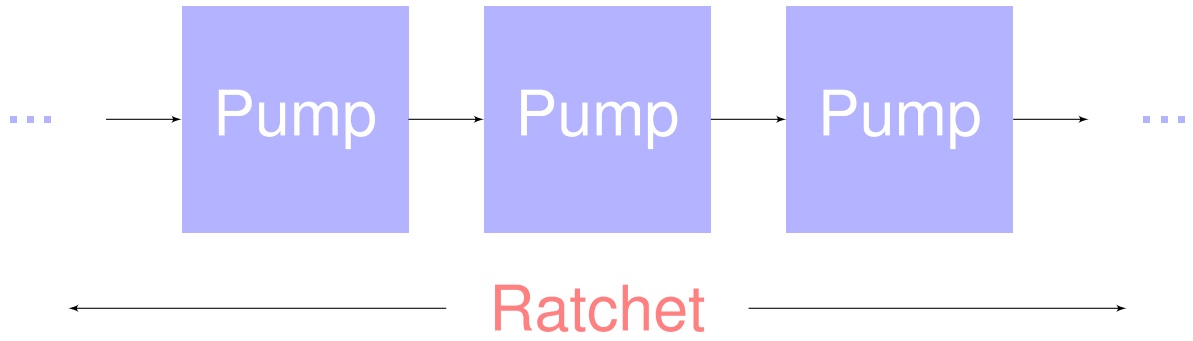

Hamiltonian ratchets [24] then consists of closed ratchets which admits a complete description via Hamiltonian dynamics. The advantages of this consists in the application of methods from deterministic dynamics to the description of the directed transport through the ratchet. As a consequence of this, is known that the directed transport phenomena implies the coexistence of regular and chaotic regions in the phase space. Beyond, the transport can be completely characterized by the topological properties of the adjacent regular regions.

The Hamiltonian formulation derives easily in the concept of quantum Hamiltonian ratchets. In this case, there exists also directed transport that persists for all times and that transits to the classical transport scenario when $\hbar$ is a small quantity in terms of the size of the invariant sets of the classical analogue system. There, the quantum transport is related to the expected value of velocity in the stationary states (evolution operator eigenstates) of the system. This makes possible to analyze the quantum transport in terms of the spectral properties of the system.

3. Classical Scenario

The purpose of this chapter is to introduce the existence of directed transport in classical Punchets. Using the elements shown in the previous chapter, is possible to sketch the informational structure of a punchet in the following way:

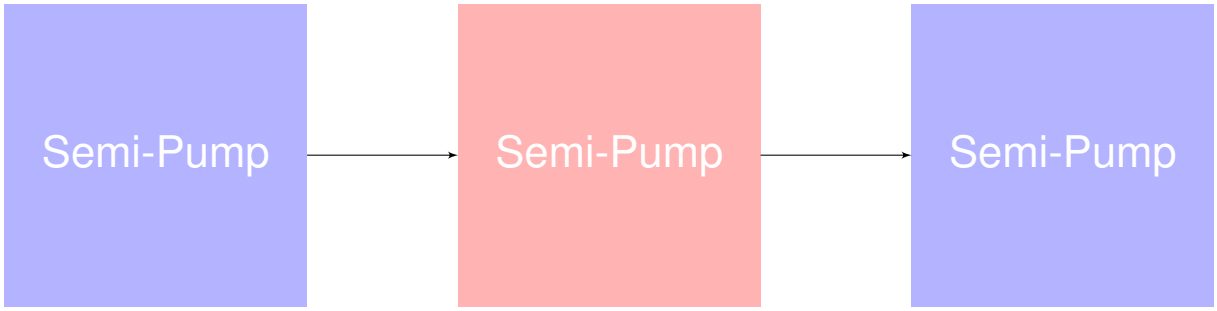

The semi-pump idea stands for an object that by itself can not generate directed transport. However, has some elements necessary for this, in particular for our case, the role of symmetry breaker. The main idea is that the semi-pumps with different color are complementary, then, the coupling of a blue semi-pump and a red semi-pump consists in total of a complete pump. Therefore, is not the isolated behaviour but the coupling between elements what will be the essential transport mechanism. Moreover, the scenario when the red semi-pump is a complete pump and the other cells in the chain are just unit cells in a symmetric periodic potential will be discussed.

The first step to this analysis, will be to introduce a model Hamiltonian system that will exemplify the main idea of mixing a pump and a ratchet, in the previous mentioned way, using a suitable embedding into the physical space of the symmetry-breaking mechanisms. Over this model, we start our analysis, centered basically in the possibility of direct transport generation and currents control manipulating different parameters in the model. The origin of this phenomena will be discussed in the framework of irregular scattering.

3.1. Classical Model

The central idea behind a possible Punchet model is to make an adequate assignation of the symmetry breaking power to each of the physical mechanisms present in the whole system. Pumps and ratchets necessarily have to break simultaneously time-reversal and parity, but in

the study of systems like those of interest for us, like locally laser irradiated condensed matter systems, is not in general the case of a global discrete-symmetry breaking but local. In this sense what we need is an scenario where the symmetries are broken but as a consequence of the mutual work of a pump and a ratchet.
The way selected in this work to attempt this is the embedding of a proto-pump into reservoirs with inner proto-ratchet structure[1]. Then, the proto-ratchet works as a supplier for the proto-pump, when one breaks the symmetry that the another can't. This now can be seen as a local controlling device (or rectifier) of the information in the asymptotical proto-ratchets. For a more specific scenario, we choose that the time-reversal symmetry only can be broken by the pump, then the asymptotic scenario is static and can only break parity.

A Hamiltonian expression for this reads:

$$H(p,x) = \frac{p^2}{2m} + V_{sta}(x) + V_{env}(x) f_{dri}(x,t)$$

Where $V_{sta}(x)$ stands for the asymptotic periodic static potential (period L), $V_{env}(x)$ the localizing potential of the embedded pump and $f_{dri}(x,t)$ the actual driving mechanism, also periodic in time (period T). For our analysis, we choose sinusoidal potentials, then:

$$V_{sta}(x) = V_{sta0}(\cos(qx) + \gamma\cos(2qx - \psi))$$

And for the envelope:

$$V_{env}(x) = \chi_{[-a,a]} V_{env0} \left(1 + \beta\frac{x}{b}\right) \exp\left[-\frac{1}{(x^2 - a^2)^2}\right]$$

Where χ_I is the characteristic function on the interval I where the time reversal symmetry is broken. This function has the property of being infinitely often differentiable. The driving could be space-dependent, what will be of interest, for example, when modeling a more realistic version of the laser-surface interaction in terms of a travelling wave confined to the pumping region. In order to define a concrete setup we use

$$f_{dri}(x,t) = f(\omega t) = \cos(\omega t) + \alpha\cos(2\omega t - \phi)$$

The central symmetry breaking mechanism in this model relies on the phases ϕ and ψ that control the time-reversal and asymptotic parity symmetries respectively, plus the β parameter that controls the parity in the driving region . For the travelling wave scenario we just make the composition

$$f_{dri}(x,t) = f_{dri}[k(x' - vt)]$$

[1] The prefix *proto* in this sentence indicates that the symmetries for actually pump and ratchet behaviour are not completely broken

With x' the coordinate on the propagation axis of the incident beam. The direction of the propagation can be calibrated using an incidence angle θ of the beam with respect to the surface normal. This can be written in the following form

$$x' = \sin(\theta)x$$

Taking x as the surface coordinate. We see that when the beam impacts the surface perpendicularly, the space dependence of the driving vanishes.

Therefore, we have three different symmetry breaking scenarios in terms of the parameters of this model:

- Type I: driving breaks space and time symmetries
  $\beta \neq 0$, $\alpha = 0$.
- Type II: asymptotic potential breaks parity with time-asymmetric driving
  $\gamma > 0$, $0 < \psi < \pi$, $\alpha > 0$, $0 < \phi < \pi$
- Type III: confined travelling waves
  $\theta \neq 0$.

We see, then, that the travelling wave model can be reduced to any of the first two types just setting $\theta = 0$ and manipulating properly the other parameters.

3.2. Dynamics

Therefore, from the Hamilton equations

$$\begin{aligned}
\dot{p} =& -\frac{\partial H}{\partial x} = V_{sta0}\left(q\sin(qx) + 2\gamma\sin(2qx-\psi)\right) - \chi_{[-a,a]}V_{env0}\left(\frac{\beta}{b}\exp\left[-\frac{1}{(x^2-a^2)^2}\right] + \right.\\
&\left.\left(1+\frac{\beta}{b}x\right)\exp\left[-\frac{1}{(x^2-a^2)^2}\right]\frac{4x}{(x^2-a^2)^3}\right)\left(\cos(k(\sin(\theta)x-vt)) + \cos(2k(\sin(\theta)x-vt)-\phi)\right) +\\
&\chi_{[-a,a]}\left(1+\beta\frac{x}{b}\right)\exp\left[-\frac{1}{(x^2-a^2)^2}\right]\left(k\sin(\theta)\sin(k(x-vt)) + 2k\sin(\theta)\sin(2k(x-vt)-\phi)\right)\\
\dot{x} =& \frac{\partial H}{\partial p} = \frac{p}{m}
\end{aligned}$$

These equations are solved numerically using a 4th order symplectic splitting method specified in Annex A. The analysis of the resulting trajectories will be done at two main stages: first, classifying the trajectories on phase space in terms of their asymptotic behaviour, that is, for a specific set of initial conditions distributed uniformely along a phase space window, determine which trajectories go away towards the asymptotic regions or, conversely, remains bounded

to some area. Second, analyzing the net currents existing in the Hamiltonian induced flow through the scattering region.

Both perspectives give insight about the chaotic phenomena manifestation and the relevance of this chaotic behaviour in terms of control of the asymptotic region information, which is the main topic of the actual work. Therefore, is essential to compare the asymptotic behaviour when scattering is turned off with the scattering influence as far as the control parameters are varying.

3.2.1. Irregular Scattering

A characteristic feature of the scattering analysis carried out in this work is the non-free asymptotic behaviour but a crystalline (period L), and possibly, parity non-invariant nature of the potential at times $t^{\pm} = \pm\infty$. This has direct implications as, for example, the existence of closed periodic trajectories out from the scattering region. In our model we have infinite potential minima as a consequence of the sinusoidal form. Then, when we were sampling initial conditions along the phase space, is important to take in account possible undesirable confination of trajectories and select only those conditions that evolve towards the scattering region. This can be expressed in terms of the total energy of each trajectory, that must be above the absolute maximum of the potential

$$E_{\pm} > \sup_{x_{\pm} \leq x_{\pm}+L} V_{sta}(x)$$

Moreover, is interesting to see how the scattering control parameters changes this structure when the scattering region overlaps some bounded asymptotic behaviour region, generating new bounded regions or destructing the asymptotic ones.

In order to observe this we generate the stroboscopic surface of section for the Hamiltonian dynamics of our model. This is just a register of successive snapshots of the dynamics in terms of the period of the driving. In figure 3-1 we take a grid of initial conditions just before the gray scattering region $(-1, 1)$, with positive momentum, that is, a collection of entering trajectories going from left to right, for the vanishing scattering scenario in the parity invariant and non-invariant case. The green color indicates that all the trajectories that enter on the scattering region are transmitted, which is trivial. Also, we plot the bounded trajectories that are the black islands in the plot.

These are put into the plot to emphasize their existence and how they progressively change its nature as a consequence of their overlap with the scattering region. Turning on the driving, that is, progressively increasing the V_{env0} value for a fixed value of the rest of parameters, we start to see the control of the flow induced by the scattering region. For the Type I, II and II models we have the results of the Fig 3-2. The arousing of chaotic phase-space structures in

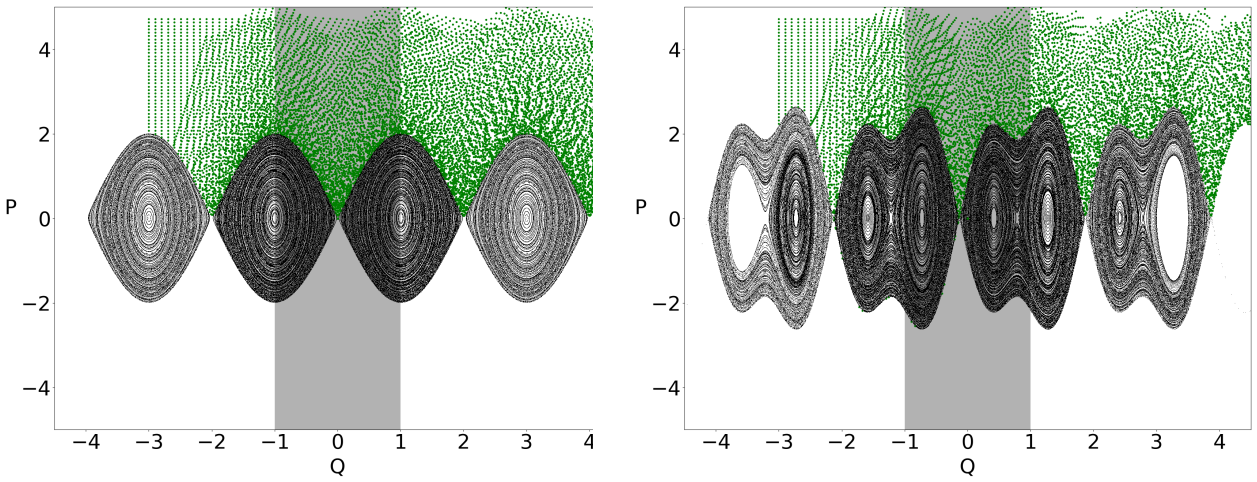

(a) Parity Invariant ($\psi = 0$)

(b) Parity Non-Invariant ($\psi = -\pi/3$)

Figura 3-1.: Asymptotic behaviour $V_{env0} = 0$. Left-to-Right dynamics.

the scattering region and in the overlapping bounded trajectory regions starts from low values of the driving intensity. The chaotic transients are typical of this scenarios, as can be seen from the accumulation of colored points in the vicinity of the induced gray chaotic structures, before they leave to the asymptotic regions. In this sense, this are examples of non-attracting chaotic sets in this case called *chaotic repellers*.

This behaviour in the stroboscopic surface of section are characteristic of irregular scattering [**?**]. This is related with the fractal structure of the invariant set (gray structures overlapping scattering region in our plots), in this case generated by the nonlinear nature of the driving. Another possible criteria for the characterization of irregular behaviour in the scattering process is the manifestation of self-similarity in deflection (also called *reaction*) functions, that are functions that relates an incoming parameter with an outcome one. For our analysis, we can plot the initial conditions Q_0, P_0 with the final ones Q_f, P_f. Some of this plots are given in Fig 3-3, showing extremely rapid oscillations where the initial conditions generate trajectories that have a lot of points in the scattering region for the stroboscopic maps. This relation between strong fluctuations and long delay times are typical from irregular behaviour. Moreover, a zoom on the plotting scale shows the characteristic self-similarity. With this, we can verify the irregular nature of the scattering in the proposed model.

In literature is also discussed the properties of the probability density $P(t)$ for a classical particle to stay in the scattering region for a time longer than t. Depending on the nature of the chaotic repeller, in terms of its hyperbolic or elliptic nature, $P(t)$ can behave in different

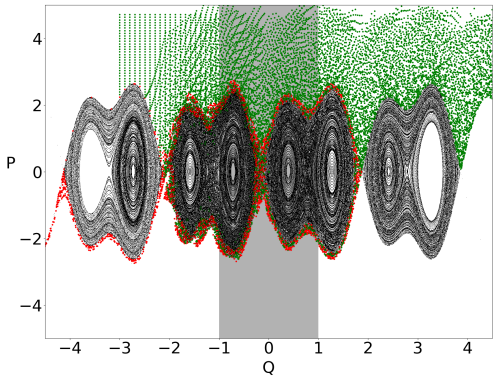

(a) $V_{env0} = 1$

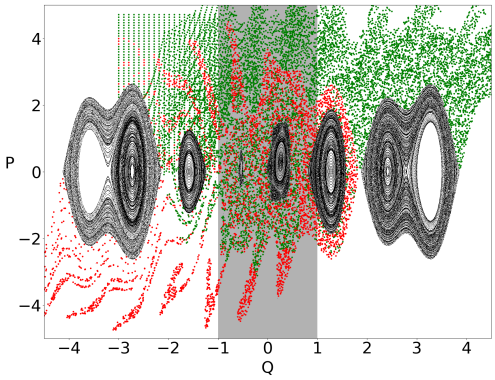

(b) $V_{env0} = 10$

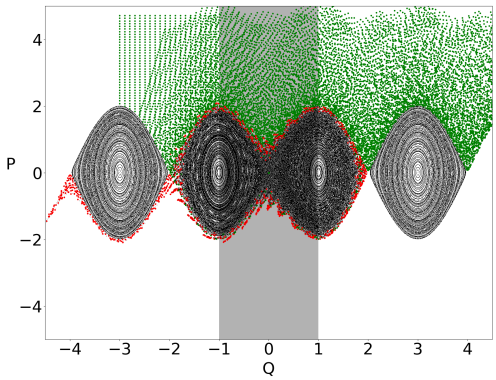

(c) $V_{env0} = 1$

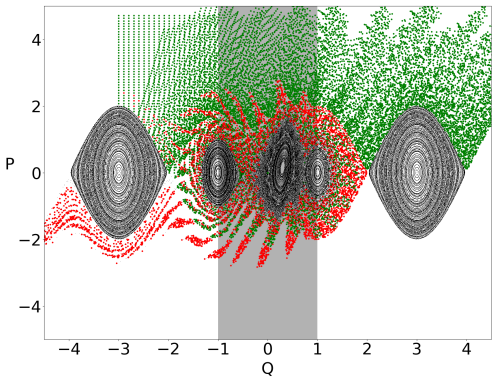

(d) $V_{env0} = 5$

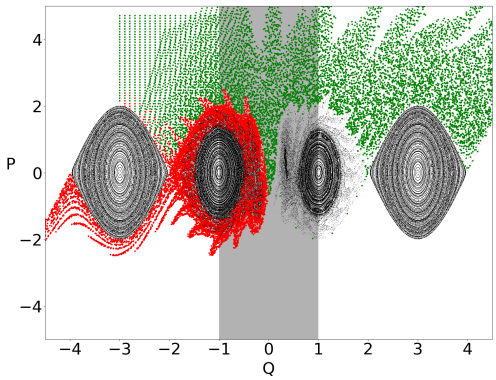

(e) $V_{env0} = 1$

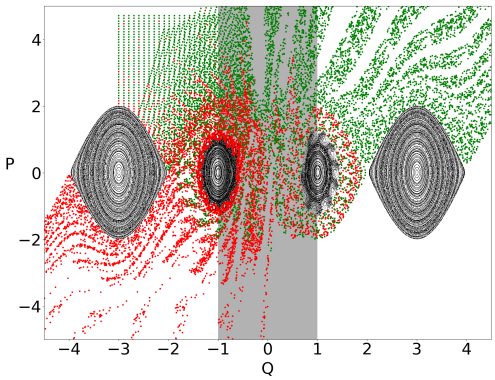

(f) $V_{env0} = 3$

Figura 3-2.: In the first row we have the Type I model with $V_{asin} = 1$ $\lambda = \pi$, $\gamma = 1$, $\psi = -\pi/3$, $\alpha = 1$, $\phi = -\pi/3$, $\omega = 2\pi$, $v = 5$. The second row is for the Type II model with $V_{asin} = 1$ $\lambda = \pi$, $\alpha = 1$, $\beta = 1$, $\phi = -\pi/3$, $\omega = 2\pi$, $v = 5$. In the last row, for Type III $V_{asin} = 1$ $\lambda = \pi$, $\alpha = 1$, $\theta = \pi/3$, $\phi = -\pi/3$, $\omega = 2\pi$, $v = 5$. In each case the non mentioned parameters vanishes.

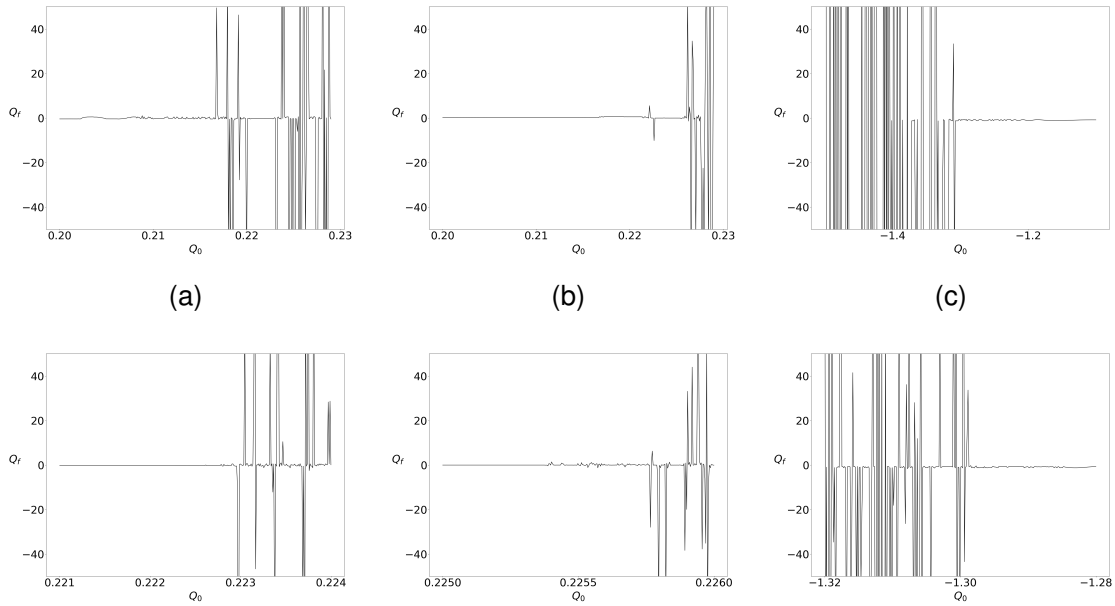

Figura 3-3.: Deflection functions for the same parameters as in the right panel of the figure 3-2. Each column represents a Type model and the second row is a zoom in the scale of the first one.

ways. When the the repeller is fully hyperbolic we have a distribution given by $P(t) \sim e^{-at}$, where a is related with the Lyapunov exponent associated to the repeller and the Haussdorf-Besicovitch dimension of the invariant set. P. Gerwinski and P.Seba [9] find an example of a repeller dominated mainly by elliptic trajectories, due to the existence of an elliptic domain on the fractal set, which induces an algebraic decay of the probability density $P(t) \sim t^{-a}$. The driving dependence of many parameters for our model, can generate different chaotic repellers, dominated by different types of trajectories, for the same asymptotic scenarios. The relevance of this for the transport analysis is not considered.

3.2.2. Directed Transport

As it was discussed during the model construction, the breaking of the parity and time-reversal symmetry are essential for the existence of net currents of some quantity in the framework of ratchets and pumping. As a central element of our proposal is the *dissociated* mechanism of symmetry breaking, conferring to each subsystem in the punchet a specific symmetry to control in terms of the above mentioned parameters. Moreover, as it was already shown via the stroboscopic surface of section, this system can manifest mixed phase space (also called inhomogeneous), in the sense that is possible to identify regular motion coexisting with the chaotic structures induced by the driving. Is well-known in literature that this manifestation is

not accidental [**?**], but a necessary condition for the existence of directed transport.
To show explicitly that this conditions indeed generates net currents we start with the usual definition of current in scattering systems introducing the quantity $T_{\alpha\beta}$ that denotes the number of particles that goes from the α to β transmission channel. In this case, the channels are just the asymptotic scenarios in our 1D scheme, that is, left and right. Furthermore, is possible also to denote the reflected fraction of particles with $R_{\alpha\alpha}$ and using this, defining the normalized current towards and specific channel in the form,

$$I_\alpha = T_{\beta\alpha} + R_{\alpha\alpha}$$

Then, the total or net current is computed as the normalized current of the positive channel (right, in terms of the coordinate system) minus the normalized current of the negative one (left),

$$I_{\text{tot}} = I_r - I_l$$

Hence, the existence of directed transport is equivalent to the non-vanishing of the previous expression for some value of the parameters in the model. One way to illustrate this in our model, is analyzing each trajectory in the simulation, associated to a specific initial condition in phase space. The method consists in the comparison between trajectories generated by an initial grid and the trajectories generated by the same grid values but inverted with respect to the diagonal in the phase space, that is, for an initial uniform distribution in the rectangle $[q_0, q_1] \times [p_0, p_1]$ we construct an uniform distribution over the area $[-q_1, -q_0] \times [-p_1, -p_0]$. The consequence of this is two families of trajectories that arrives to the scattering region in symmetric conditions. Therefore, if there is any symmetry breaking induced by the scattering, this can be registered comparing symmetric pairs.
Then, we compare the trajectories with the same absolute value of position and momentum using the following criteria:

- If both trajectories ends in the right channel, we associate a +1 to the pair.
- If both trajectories ends in the left channel, we associate a -1 to the pair.
- Otherwise, we associate a 0 to the pair

Finally, we plot the absolute value of the initial grid, putting in each coordinate the assigned value via the color code +1/green, -1/red, 0/white. The results of this are showed in the figure 3-4 for the same parameter values than in the figure 3-2. The existence of colored regions proofs the manifestation of asymmetrical behaviour induced by the driving.

Is of particular interest the appearance of fractal structures in the boundaries between the green and red regions. This behaviour is similar to the basins of attraction in the strange attractors scenario. The reason of this is that the only difference between a chaotic repeller and a strange attractor is the mechanism that underlies the creation of the invariant set. While the

attractor is generated by contraction due to dissipation, in the repellers the set is generated by leakage from a specific region, in this case, the scattering region. Therefore, the analogue of the basins of attraction for the repellers are the plots of figure 3-4.
As in the strange attractors the fractal boundaries between the regions are characteristic from chaotic motion, so this is more evidence in favour of the irregular nature of the dynamics in this model

3.2.3. Currents and Symmetries

The previous mentioned features of the model, in terms of symmetry breaking and mixed structures in phase space, indicates that this system shows a privileged direction for the particle motion. Therefore, the existence of directed currents in some regions of phase space are naturally expected.

However, one of the main points of the punchet is the particular way it generates the symmetry breaking via tunable parameters in an experimental configuration. Therefore, we only not look for directed currents but the dependence of this currents of the symmetry parameters in the model. This is equivalent to reconstruct the general expression:

$$I_{tot} = T_{tot}(\phi, \psi, \beta, \theta)$$

This is interesting in terms of experimental control, specially talking about time-reversal breaking, because the parameters that control this symmetry are confined to the scattering region. In this sense, we can manipulate currents globally just changing local information about the scatterer.

Depending on the model type, we have specific parameter dependences that regulate the current generation. Then, for Type I models the parity symmetry depends only of the ψ phase, but the tyme-reversal symmetry is controlled by the ϕ phase of the driving. Then, in this models, is sufficient to study the current dependence of this quantities. This is show in figure 3-5. There we note expected inversions of the current in the form

$I(\psi, \phi) = -I(-\psi, \phi)$

When we invert the ϕ phase, however, we found a change in the intensity of the net current but not a total inversion, if the intensity of the driving remains the same. In other hand, if we modify the intensity, it is possible to generate the desired current inversion for a specific absolute value of ϕ. This shows that in the Type I model there is a relation between driving phase and intensity that controls the reversal mechanism.

For the Type II models, both breaking parity and time-reversal parameters are controlled by

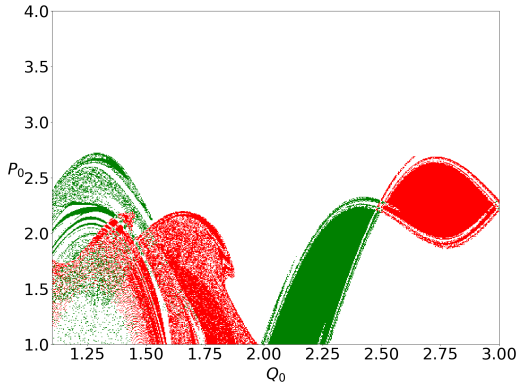

(a) $V_{env0} = 1$

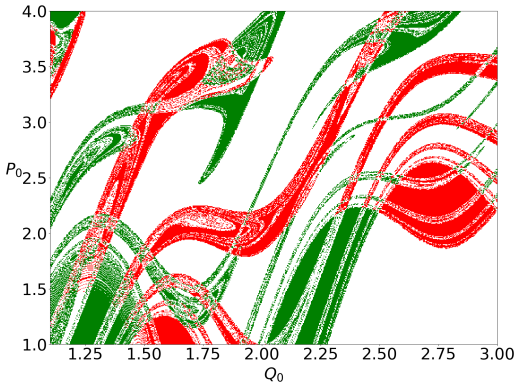

(b) $V_{env0} = 10$

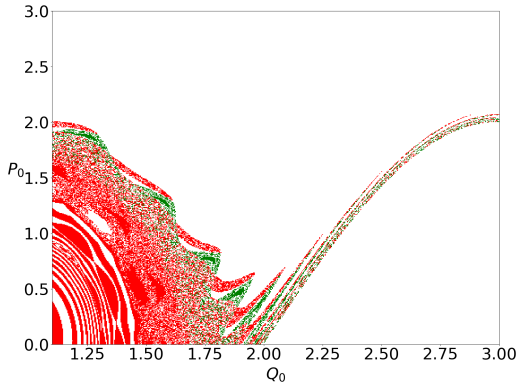

(c) $V_{env0} = 1$

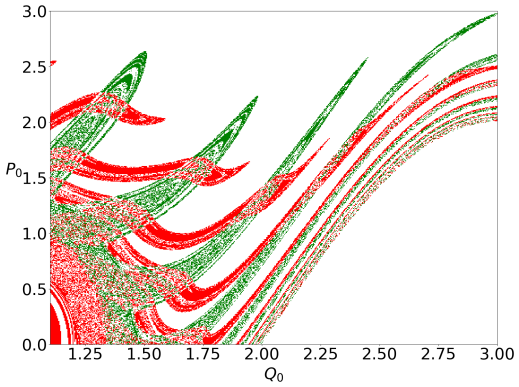

(d) $V_{env0} = 5$

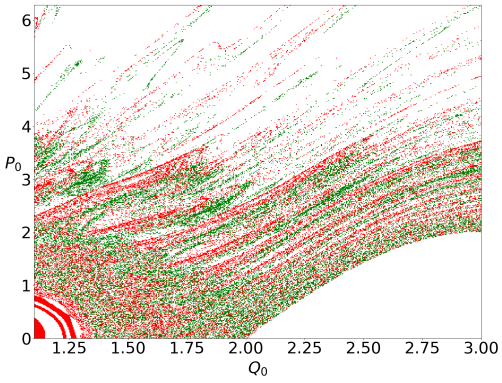

(e) $V_{env0} = 1$

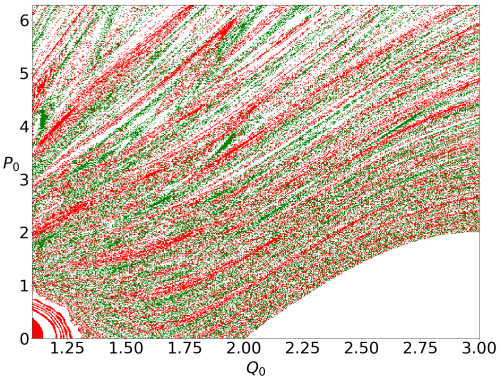

(f) $V_{env0} = 3$

Figura 3-4.: Here are the individual contributions to the transport. The colors indicate the predilected direction of the pairs of trajectories with the same absolute value of initial conditions. The parameters are the same as in the Figure 3-2.

the scattering region. There, we have parity regulated by the β parameter and time-reversal by the phase ϕ. The results are shown in the figure 3-6. Here, we saw that also:

$I(\beta, \phi) = -I(-\beta, \phi)$
$I(\beta, \phi) = -I(\beta, -\phi)$

We see, as a direct consequence that for $\phi = 0$ there can be no current. In this sense we see that for the parameter space (β, ψ, ϕ) we have inversion of currents for each axis inversion in the planes generated when one of the coordinates is equal to zero. For Type III models in figure 3-7 we have now a spatial dependence explicit in the scattering region. Then, the control of the symmetries are regulated by the argument of the cosines in the driving. A direct consequence of this is that we can not factorize the time-reversal and parity symmetry, in terms of its dependence of the parameters. Then we have that:

$$I(\theta, \phi) = -I(-\theta, \phi)$$

While the ϕ parameter just change the intensity of the currents but is not capable by itself of generate a current inversion.
In this sense we have only one separatrix between the positive and negative current regions.
An interesting scenario that arose after this analysis is when we not look for current generation but for inversion of an existent one. That is, if we have a system that already has net currents, the scattering punchet mechanism can work as a current direction switch. In figure 3-8 we show for the first panel a Type I model at $\theta = 0$ that is controlled switching on the θ parameter, showing inversions in different ranges. This proves the possibility of use one pumping parameter to control an already functional punchet. In the second panel we make the same but in a Type II for $\psi = 0$ that is controlled continuously varying the phase ψ, getting also current inversions.

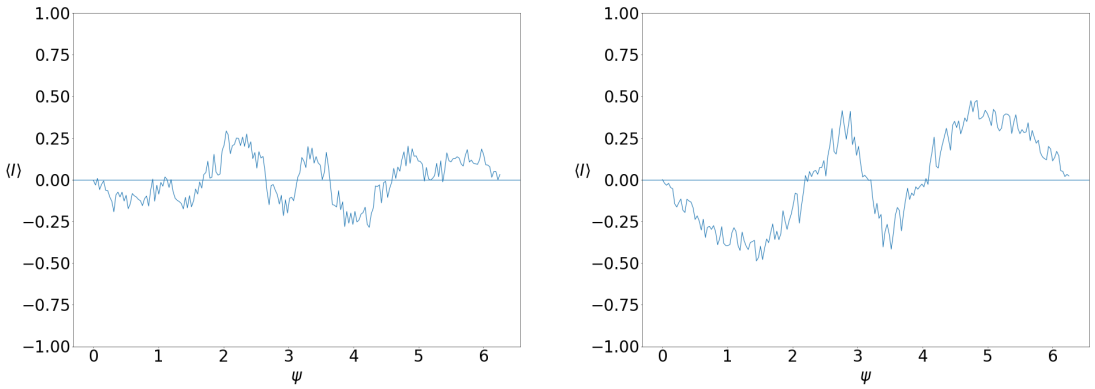

(a) $\phi = \pi/3$

(b) $\phi = -\pi/3$

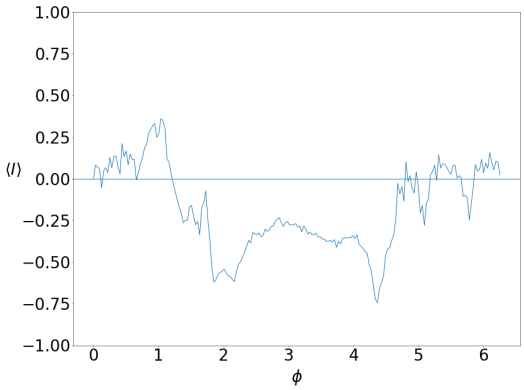

(c) $\psi = -\pi/3$

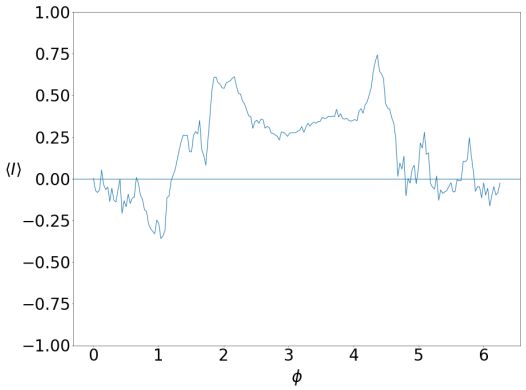

(d) $\psi = \pi/3$

Figura 3-5.: Type I Net Currents

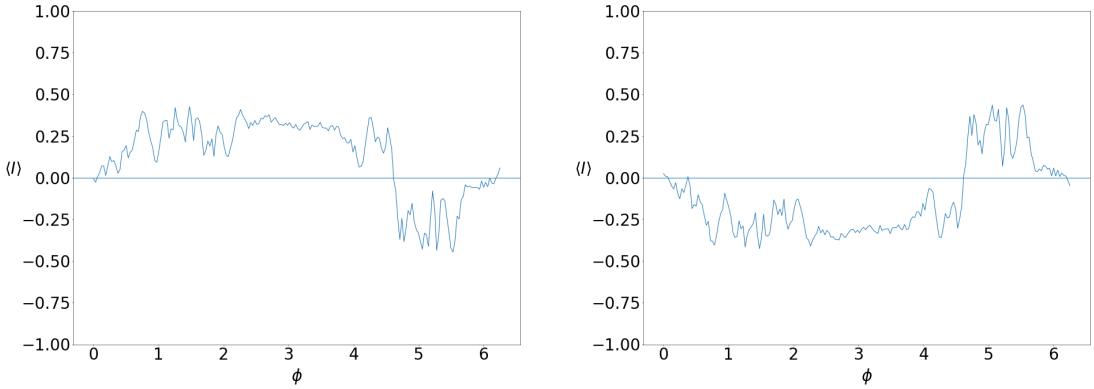

(a) $\beta = 1$

(b) $\beta = -1$

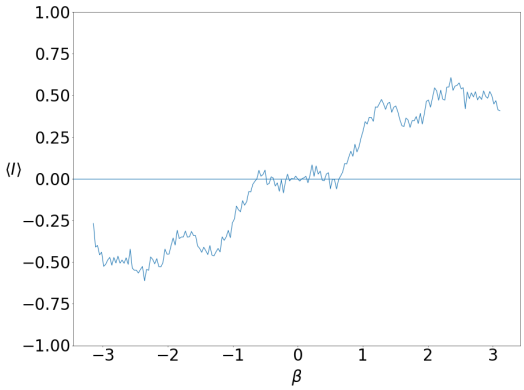

(c) $\phi = \pi/3$

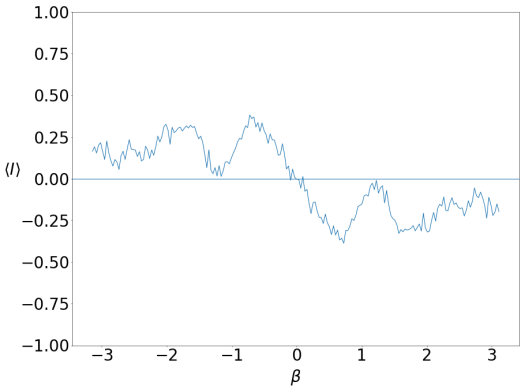

(d) $\phi = -\pi/3$

Figura 3-6.: Type I Net Currents

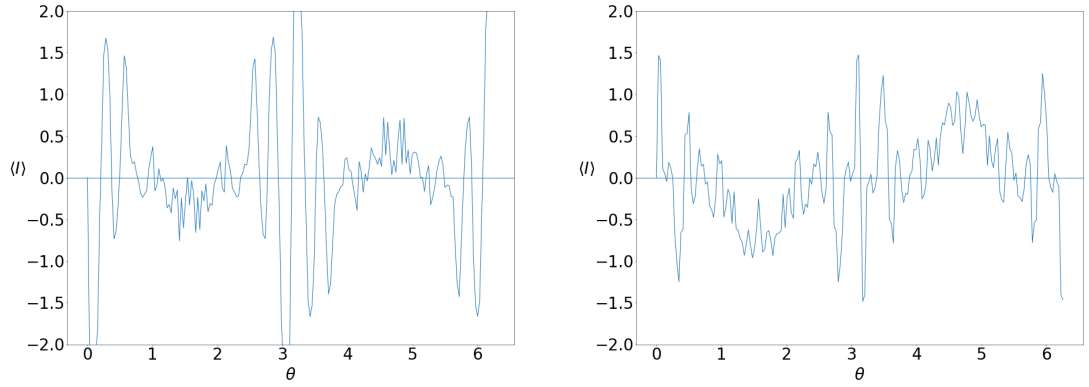

(a) $\phi = \pi/3$

(b) $\phi = -\pi/3$

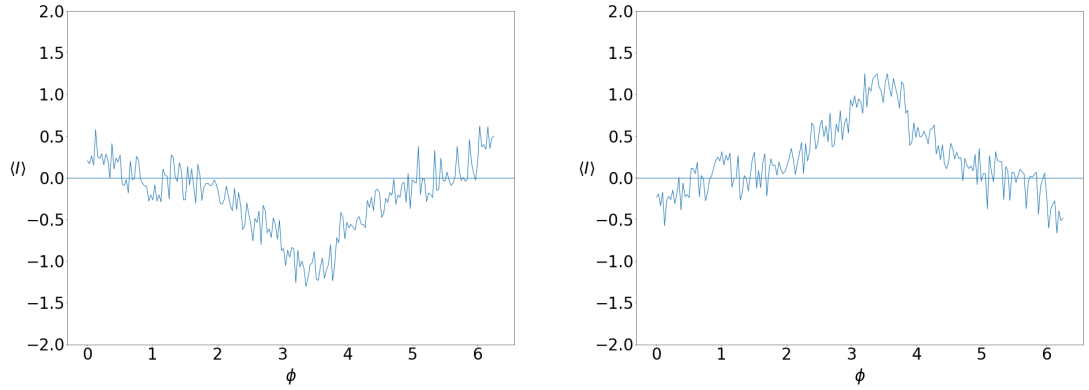

(c) $\theta = \pi/3$

(d) $\theta = -\pi/3$

Figura 3-7.: Type III Net Currents

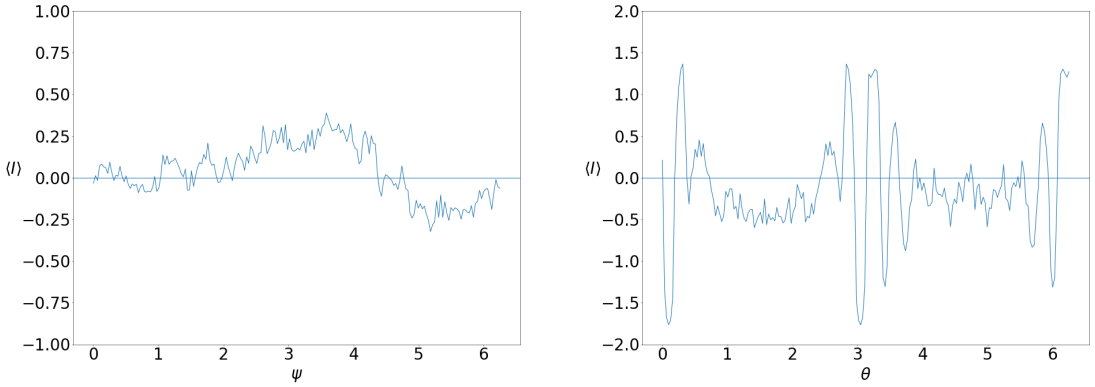

(a) Type II reversed by ψ

(b) Type I reversed by θ

Figura 3-8.: Current Reversals

4. Quantum Scenario

This chapter consists in the introduction and discussion of the quantum version of punchets. At the first stage, we see that the quantum dynamics for this class of systems are governed by a time-dependent Schrödinger equation. Furthermore, the periodicity existing in both space and time implies that this will be also well described by a hybrid mechanism between Bloch and Floquet methods (Appendix B). Therefore, in the first part of this chapter, we introduce the band structure and average momenta for the asymptotic spatially periodic scenarios in the punchet. This of essential importance because it is one of the main differences between the usual scattering systems (asymptotically free) and the punchet model.

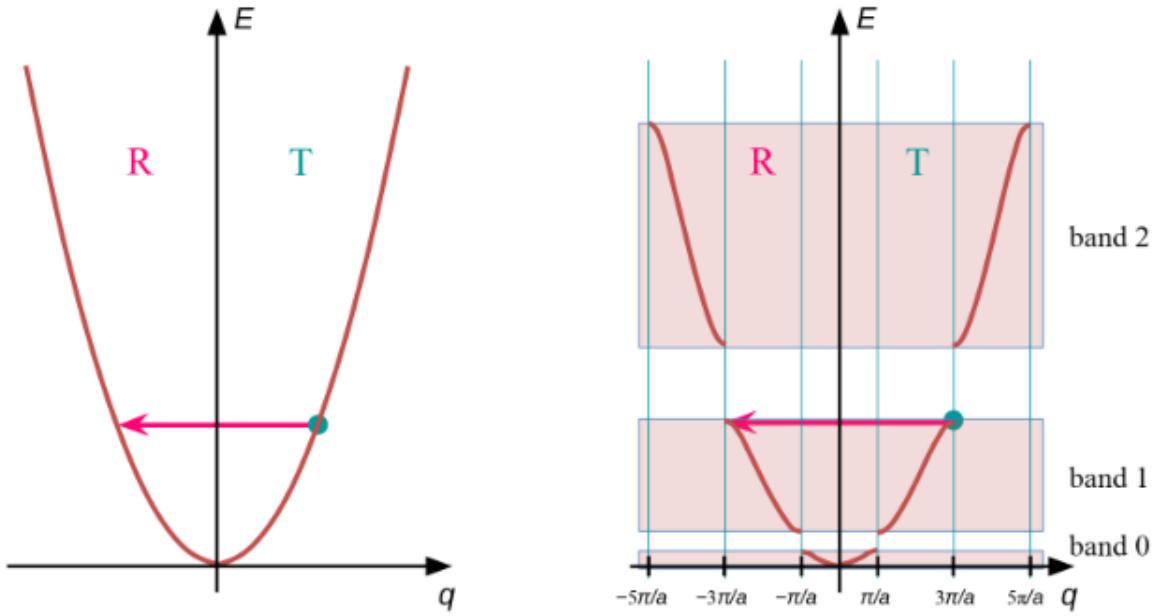

(a) Free Scattering

(b) Punchet Scattering

Figura 4-1.: Contrast between asymptotic quantum structures

After this, we can now present the wave-packet generation and propagation through the scattering region. For us, is important to characterize in which moment the incident wave-packet leaves completely the scattering region after the interaction, so we show the Husimi-Kano representation of the incident wave-packet as a possible tool to graphically determine this regime. Through this, we also introduce the possibility, for further work, of a comparison between

quantum phase-space dynamics and classical phase-space structures. This will lead to semi-classical analysis in terms of the expected localization of states in the invariant set generated by the driving when $\hbar \to 0$ [2].

Finally, we show how the punchet mechanism, specifically couples the time periodicity and the spatial periodicity, showing the energy shifts that the transmitted and reflected wave-packets manifests in the band structure of the asymptotic system, with respect to the incident one, due to the Floquet shifts that the quasimomentum suffers in the interaction.

4.1. Asymptotic Band Structure

For the analysis of the band structure we make a diagonalization of the Hamiltonian matrix written in a typical base of well-defined momentum wave functions, that is, plane waves. The truncation of the Hamiltonian is made at 251 modes, where we find expected dynamical behaviour as it will be shown in the next section. So, starting from a general asymptotic scenario

$$V_{asin}(x) = V_{asin0}(\cos(\lambda x) + \gamma \cos(2\lambda x - \psi))$$

We solve the Schrödinger equation using the ansatz shown in the Appendix B,

$$\psi(x) = \sum_{n\in\mathbb{Z}} a_n e^{in\lambda x}$$

Then,

$$\sum_{n\in\mathbb{Z}} \left[\frac{\hbar^2\lambda^2 n^2}{2m} e^{in\lambda x} + V_{asin0}\left(e^{i\lambda(n+1)} + e^{i\lambda(n-1)} + \gamma e^{i(\lambda(n+2)-\psi)} + \gamma e^{i(\lambda(n-2)+\psi)} \right) \right] a_n = E \sum_{n\in\mathbb{Z}} e^{i\lambda nx} a_n$$

Multiplying by the factor $\frac{\lambda}{2\pi} e^{-i\lambda nx}$ and performing the integral over a period, the previous equation results in:

$$\frac{\hbar^2\lambda^2 n^2}{2m} a_n + V_{asin0}\left(a_{n-1} + a_{n+1} + \gamma e^{-i\psi} a_{n-2} + \gamma e^{i\psi} a_{n+2} \right) = E a_n$$

Which shows how contiguous Fourier components couples. We can restate this in terms of the quasimomentum in the form,

$$n = k + m\lambda$$

With $m \in \mathbb{Z}$ and $k \in (-\frac{\lambda}{2}, \frac{\lambda}{2})$. Then, the previous expression is restated as

$$\frac{\hbar^2\lambda^2 (k+m\lambda)^2}{2m} a_m^k + V_{asin0}\left(a_{m-1}^k + a_{m+1}^k + \gamma e^{-i\psi} a_{m-2}^k + \gamma e^{i\psi} a_{m+2}^k \right) = E a_m^k$$

So, this is basically an eigenvalue problem of the form:

$$\mathcal{M} = \begin{pmatrix} \vdots \\ a_2^k \\ a_1^k \\ a_0^k \\ a_{-1}^k \\ a_{-2}^k \\ \vdots \end{pmatrix} = E \begin{pmatrix} \vdots \\ a_2^k \\ a_1^k \\ a_0^k \\ a_{-1}^k \\ a_{-2}^k \\ \vdots \end{pmatrix}$$

Where:

$$\mathcal{M} = \begin{pmatrix} \ddots & \cdots & \cdots & \cdots & \cdots & \cdots & \ddots \\ \cdots & \frac{\hbar^2(k+2\lambda)^2}{2m} & \frac{1}{2}V_{asin0} & \frac{\gamma}{2}V_{asin0}e^{-i\psi} & 0 & 0 & \\ \cdots & \frac{1}{2}V_{asin0} & \frac{\hbar^2(k+\lambda)^2}{2m} & \frac{1}{2}V_{asin0} & \frac{\gamma}{2}V_{asin0}e^{-i\psi} & 0 & \\ \cdots & \frac{\gamma}{2}V_{asin0}e^{i\psi} & \frac{1}{2}V_{asin0} & \frac{\hbar^2k^2}{2m} & \frac{1}{2}V_{asin0} & \frac{\gamma}{2}V_{asin0}e^{-i\psi} & \\ \cdots & 0 & \frac{\gamma}{2}V_{asin0}e^{i\psi} & \frac{1}{2}V_{asin0} & \frac{\hbar^2(k-\lambda)^2}{2m} & \frac{1}{2}V_{asin0} & \\ \cdots & 0 & 0 & \frac{\gamma}{2}V_{asin0}e^{i\psi} & \frac{1}{2}V_{asin0} & \frac{\hbar^2(k-2\lambda)^2}{2m} & \\ \ddots & \cdots & \cdots & \cdots & \cdots & \cdots & \ddots \end{pmatrix}$$

As it was mentioned at the beginning of the chapter, we choose a truncation such that the *Bloch Matrix* $\mathcal{M}$ has dimensions 251×251. Then, for each quasimomentum value, we have a total of 251 different eigenvalues that will be written as $E_n(k)$, where n is the index of the eigenvalue and is called the *band index*. These eigenvalues are continuous functions of k. The set of energies for a fixed n value is precisely what is called an *energy band*. For the 2 different asymptotic potentials that appear in the model Types of punchets, we show in Figure 4-2 the band structure of each one, indicating a specific state with a red point. The colors stand for different energy bands. Moreover, the energy eigenstates are written in terms of the eigenvectors in the previous eigenvalue problem. The *Bloch functions*, as it is presented in the appendix, then has the form:

$$\phi_{nk}(x) = e^{ikx}u_{nk}(x)$$

Where,

$$u_{nk}(x) = \sum_{n\in\mathbb{Z}} a_n^k e^{in\lambda x}$$

It is possible to derive a dynamical equation for the $u_{nk}(x)$ terms, replacing the Bloch functions in the Schrödinger equation and discarding the phase quasimomentum terms. This equation for a general potential is stated as [6]:

$$\left[-\frac{\hbar^2}{2m}\left(\frac{\partial}{\partial x} + ik\right) + V(x)\right] u_{nk}(x) = E_n(k)u_{nk}(x)$$

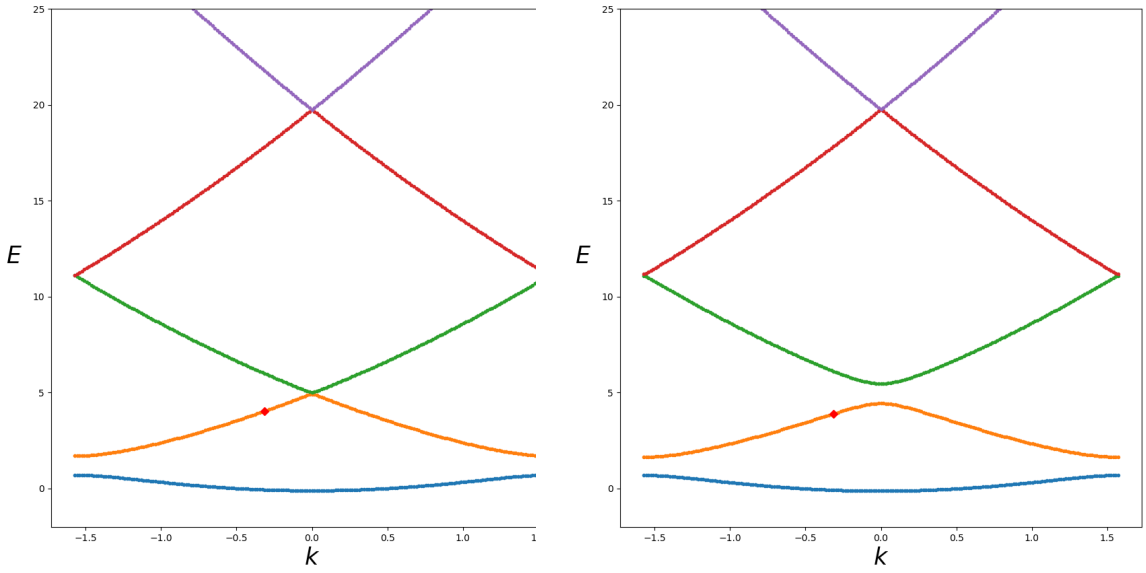

(a) Symmetric (b) Non-Symmetric

Figura 4-2.: Band Structure

Using this equation we can derive a useful formula for the expectation value of the momentum associated to a Bloch state. Taking at left the derivative $\frac{\partial}{\partial k}$, multiplying by $u^*_{nk}(x)$ and integrating over the complete domain of the functions,

$$\frac{\hbar}{m}\int u^*_{nk}\left(-i\hbar\frac{\partial}{\partial x}+hk\right)u_{nk}+\int u^*_{nk}\left(\frac{\partial u_{nk}}{\partial k}\right)=\int u^*_{nk}\left(\frac{\partial E_n(k)}{\partial k}\right)u_{nk}+\int E_n(k)u^*_{nk}\left(\frac{\partial u_{nk}}{\partial k}\right)$$

Noting that the second terms in each side cancels, we finally get,

$$\frac{\hbar}{m}\int u^*_{nk}\left(-i\hbar\frac{\partial}{\partial x}+hk\right)u_{nk}=\frac{\partial E_n(k)}{\partial k}$$

Where we take in account that,

$$-ih\frac{\partial}{\partial x}\psi_{nk}(x)=-i\hbar\left(ike^{ikx}u_{nk}(x)+e^{ikx}\frac{\partial u_{nk}(x)}{\partial x}\right)=\left(-i\hbar\frac{\partial}{e}^{ikx}\partial x+\hbar k\right)u_{nk}(x)$$

Therefore, the previous integral expression is equivalent to the expected value of the momentum for each Bloch state. These results are shown in Figure 4-3. There, we identify the same state as in the previously shown band structures, and also the same color code for the band identification

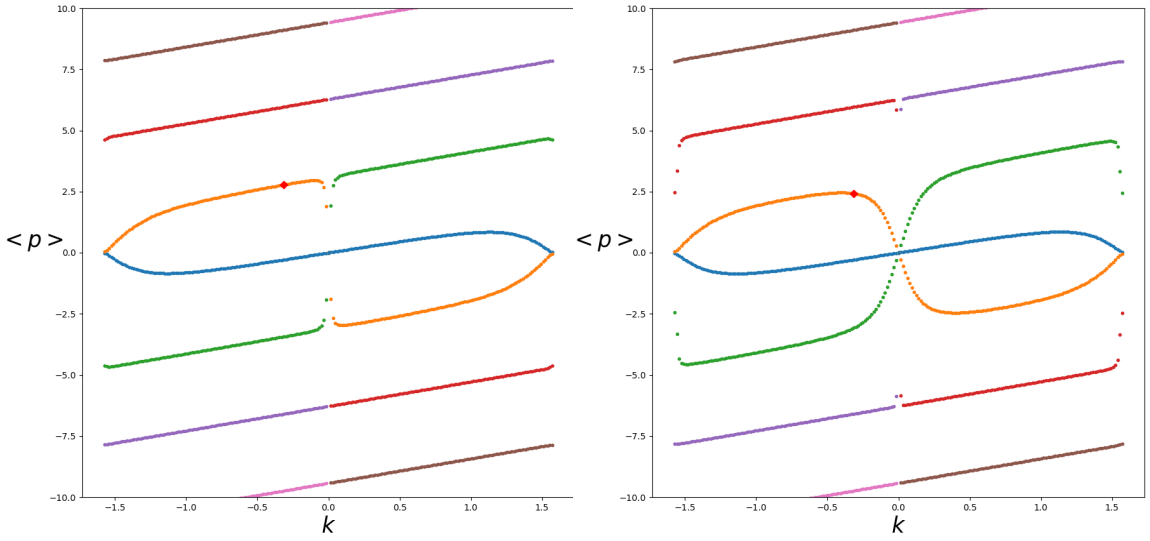

(a) Symmetric (b) Non-Symmetric

Figura 4-3.: Average Momentum

4.2. Quantum Dynamics

Now, using the numerical approach explained in Appendix A, is possible to show the evolution of an initial wave-packet through the scattering region. We are interested mainly in states that do not change its form as they travel through the asymptotic region. However, this states are precisely the Bloch functions introduced in the previous section. This energy eigenstates are *extremely* delocalized, so, in principle, is impossible to construct asymptotic wave-packets with this characteristics. A way to surpass this problem is just approximating this asymptotic wave-packet, localizing a Bloch state with a Gaussian pulse. For a sufficiently wide Gaussian, this wave-packet does not change its form as it evolves through the asymptotic region for reasonable time scales.

In Figure 4-4 we show the evolution of a wavepacket generated by the Bloch state identified by the red point in the free diagrams, times a suitable Gaussian,

$$\psi^0_{nk}(x) = \psi_{nk} \exp\left(\frac{1}{2}\frac{(x-x_0)^2}{2\sigma^2}\right)$$

Through the asymptotic potential. This verifies that the wave-packet preserve its form along the evolution on the asymptotic scenario. Here is natural to ask about the relevance of the boundary conditions of the propagation, taking in account that being a scattering system will imply, in computational terms, the existence of wave-packets further than the memory limits. In this

type of systems we can avoid partially this problem assuming a very small scattering region in comparison with the wide of the initial wave-packet. In our case, the scattering region will not comprise more than one or two unit cells of the domain in terms of the period of the asymptotic potential, but the average width of the incident wave-packet will extend to 60 or 80 unit cells.

The validity of the numerical propagation for the 4th order splitted propagator exposed in the Appendix A, was tested with typical benchmark potentials as the harmonic oscillator and the Morse potential, in terms of the (non) evolution of its stationary states. Moreover, the computational dynamics was also tested with the exact solution of the asymptotic potential when $\psi = 0$, that consists in the so called *Mathieu functions*, showing also stationary evolution without noise for long evolution times.

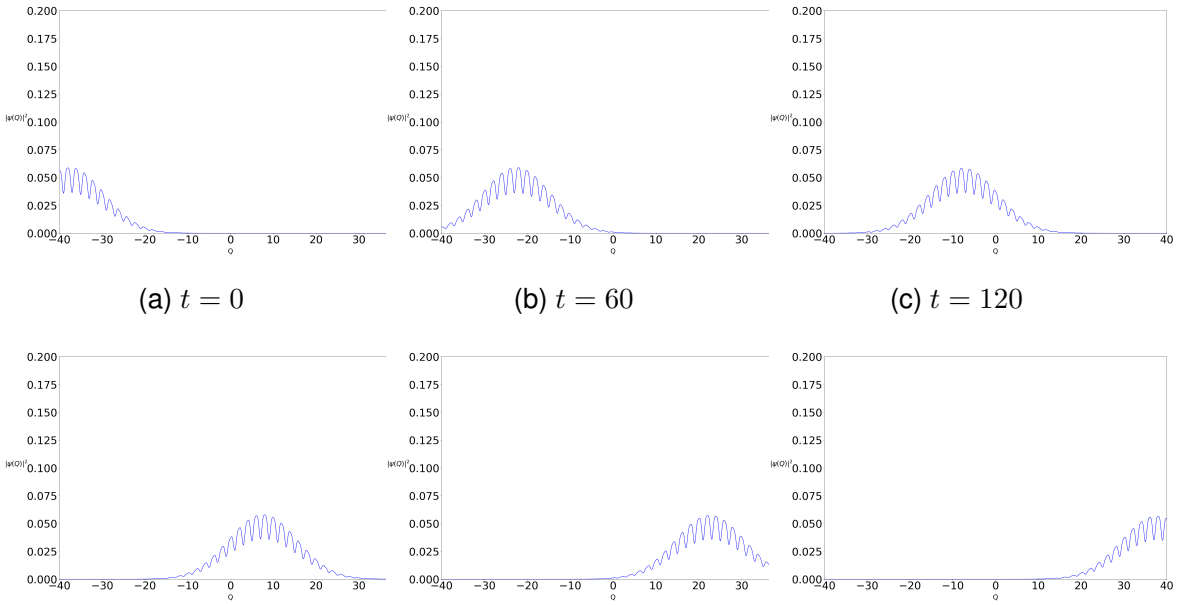

(a) $t = 0$ (b) $t = 60$ (c) $t = 120$

(d) $t = 180$ (e) $t = 240$ (f) $t = 300$

Figura 4-4.: Free propagation (symmetric)

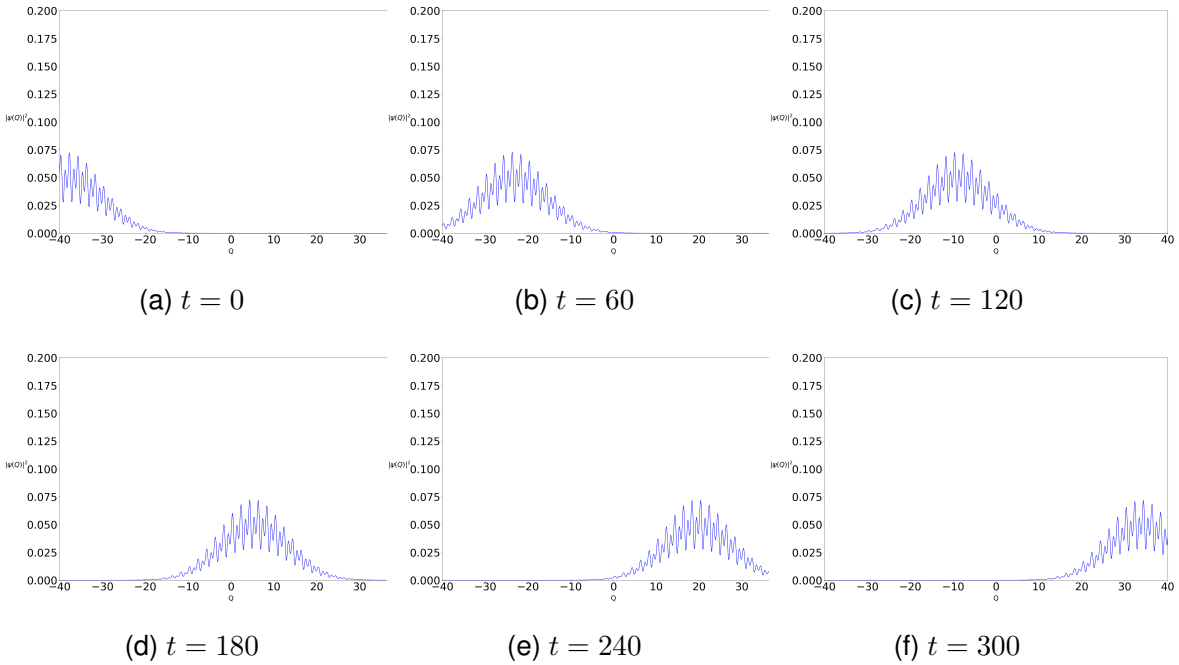

(a) $t = 0$ (b) $t = 60$ (c) $t = 120$

(d) $t = 180$ (e) $t = 240$ (f) $t = 300$

Figura 4-5.: Free propagation (asymmetric)

Now, we turn on the scattering region for the three different model types. Is important that the incident wave-packet does not overlap the driving interval. The usually selected states to be scattered belongs to the second and third band[1] as the red point state, due to its average momentum value, that makes possible to study the scattering process without very long computational times. States in upper bands propagates almost ballistically, feeling the driving more as a subtle perturbation and not interesting in our work.
For the figures 4-6, 4-7 and 4-8, the scattering region consists of the central 4 periods of the asymptotic potential, while the initial wave-packet spreads more or less 50 cells.

[1] For parameters in the scale shown through the work.

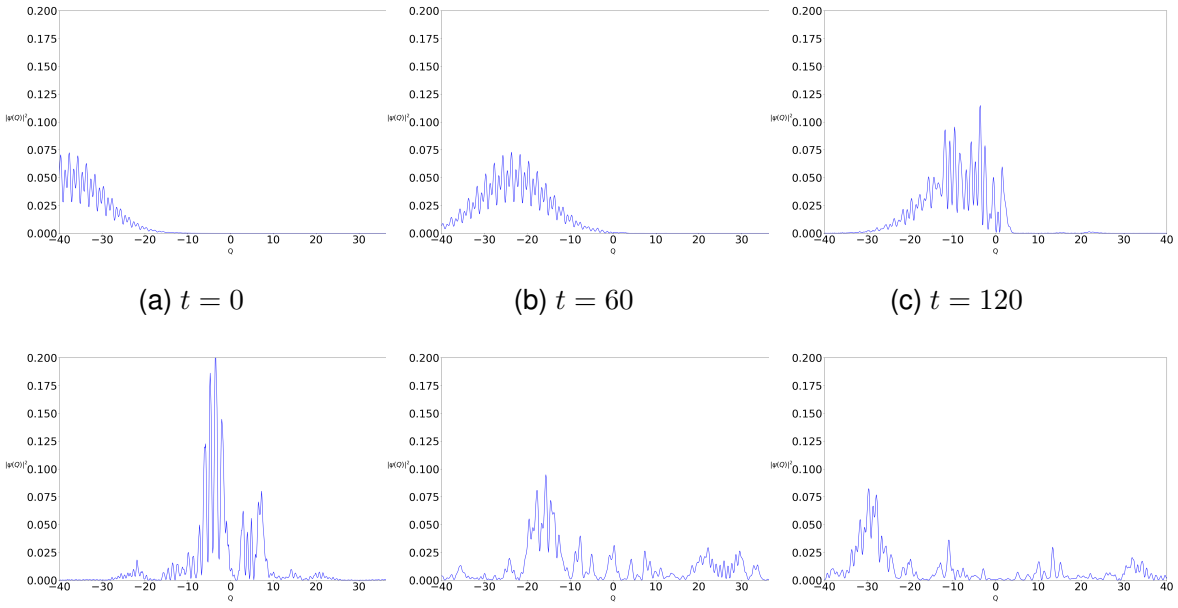

(a) $t = 0$ (b) $t = 60$ (c) $t = 120$

(d) $t = 180$ (e) $t = 240$ (f) $t = 300$

Figura 4-6.: Type I Propagation

4.3. Phase-Space Representation

In this section we introduce a possible phase space representation for the states through its scattering process. This will be helpful determining when the interaction between the incident wave-packet can be considered negligible, which is essential to the asymptotic analysis of the scattered spectra. This tool, however, can be used to study in detail the semi-classical features that makes possible directed transport, taking in account that this kind of behaviour in quantum ratchets[24] are strongly related with its analogue classical ratchet system[15]. This particular study is leave for a posterior work.

4.3.1. Q Representation

The Husimi-Kano Q function, for a pure quantum state $|\psi\rangle$ is defined as:

$$Q(\alpha) \equiv \frac{1}{\pi} |\langle \alpha | \psi \rangle|^2$$

Where $|\alpha\rangle$ is a coherent state of the harmonic oscillator, indexed by the complex quantity α. Therefore, the Q function depends on the real and imaginary parts of α, which will define the coordinates in the phase-space associated to the Q function. This representation has the property of being positive everywhere in phase-space, in contrast with the Wigner representation

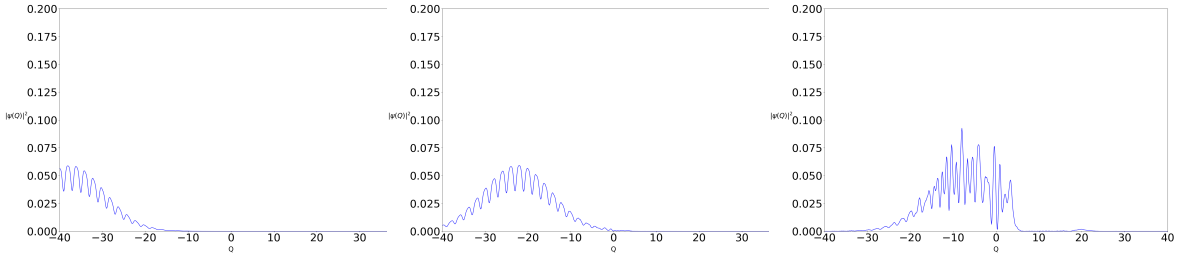

(a) $t = 0$ (b) $t = 60$ (c) $t = 120$

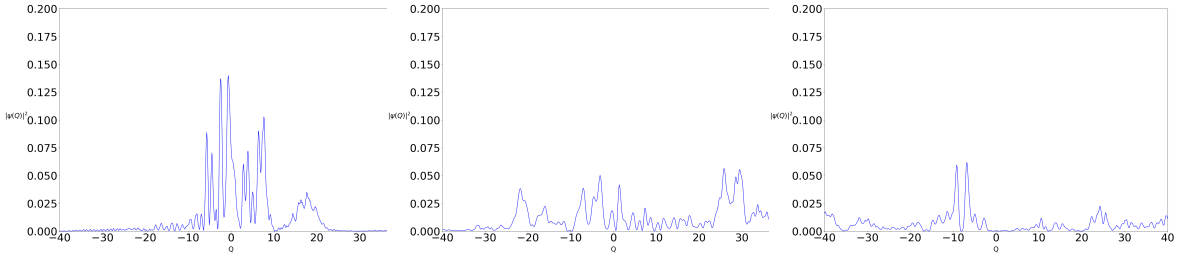

(d) $t = 180$ (e) $t = 240$ (f) $t = 300$

Figura 4-7.: Type II propagation

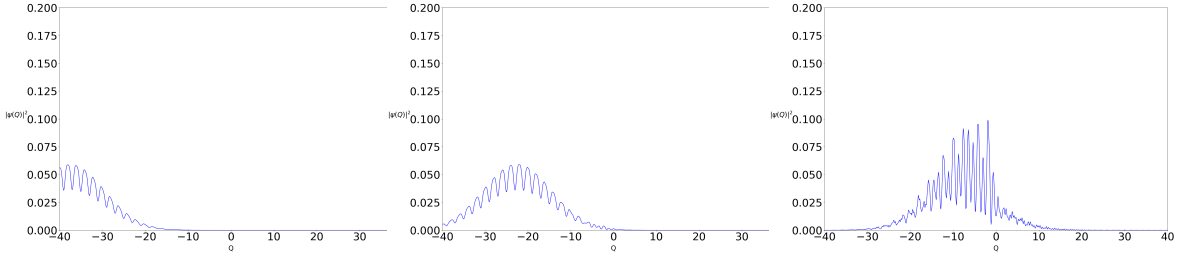

(a) $t = 0$ (b) $t = 60$ (c) $t = 120$

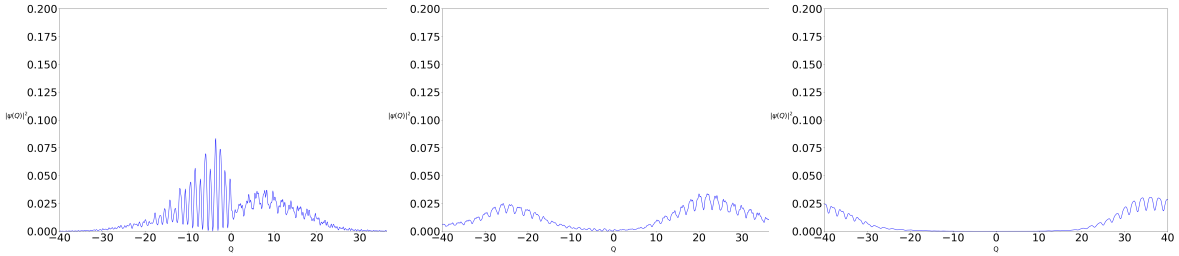

(d) $t = 180$ (e) $t = 240$ (f) $t = 300$

Figura 4-8.: Type III propagation

that can show negative values in some cases. Also, this two representations are related via a *Weierstrass transform*:

$$Q(\alpha) = \frac{2}{\pi} \int W(\beta) e^{-2|\alpha-\beta|^2} d^2\beta$$

4.3.2. Examples

Here we show how the red point states behave in its Husimi-Kano representation, under scattering for the 3 types of models.

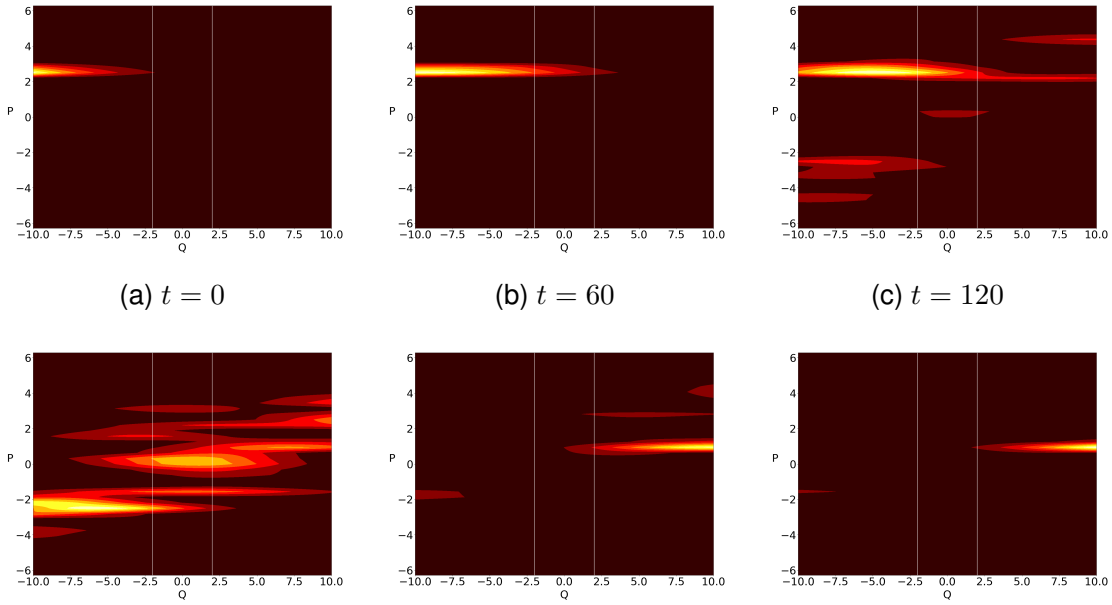

(a) $t = 0$ (b) $t = 60$ (c) $t = 120$

(d) $t = 180$ (e) $t = 240$ (f) $t = 300$

Figura 4-9.: Type I Propagation

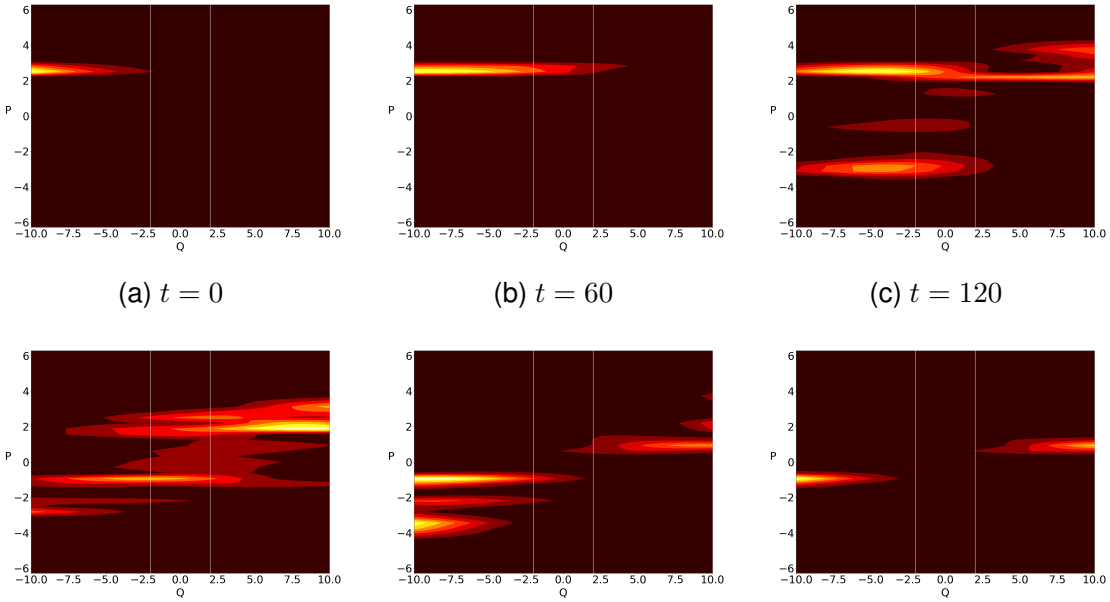

(a) $t = 0$ (b) $t = 60$ (c) $t = 120$

(d) $t = 180$ (e) $t = 240$ (f) $t = 300$

Figura 4-10.: Type II propagation

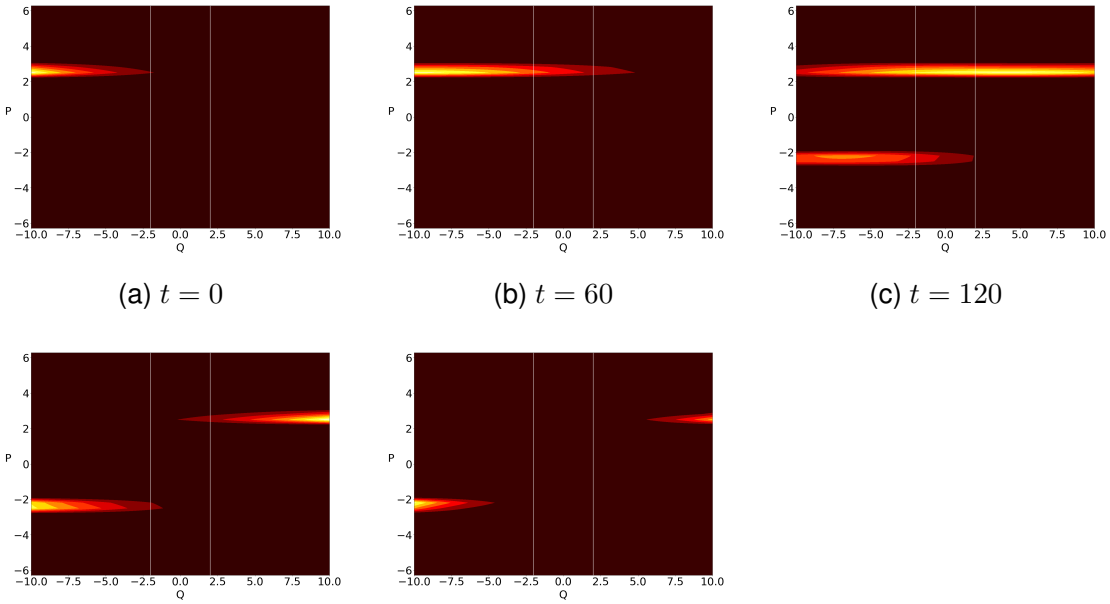

(a) $t = 0$ (b) $t = 60$ (c) $t = 120$

(d) $t = 180$ (e) $t = 240$

Figura 4-11.: Type III propagation

4.4. Scattering Diagrams

In order to understand how the incident wavepacket scatters towards the asymptotic regions, we look for the projection of the final state in the asymptotic band states. That is, we have to compute the quantities:

$$|\langle\psi_R(t\to\infty)|\psi_{nk}\rangle|^2, \qquad |\langle\psi_T(t\to\infty)|\psi_{nk}\rangle|^2$$

That stands for the transition probabilities between the reflected (R) and transmitted (T) wave-packets, and the Bloch functions. This reflected and transmitted components are found when the systems evolve for a long period of time. Computationally, this time is taken just the necessary for the both wave-packets leave completely the scattering region.

Now, we know via Floquet theory that the energy through the scattering process is preserved modulo a photon shift $\hbar\omega$, where ω is the driving frequency. Therefore, in general terms, the scattered wave-packet will be a combination of modes corresponding to different Bloch states, each one associated to an energy shift resulting of the integer interchange of photons with the driving. So, the main question in this point relies on the energy scales between the energy induced by the driving, at each photon, and the dimensions of the bands. If the frequency of the driving is too high, the wavepacket will jump between bands, but if the driving is adiabatic, the wave-packet will remain at the same energy band.

However, strong intensities of the driving can also take a wave-packet out of its original band. For low frequencies but strong driving amplitudes is possible that the incident wave-packet absorb a sufficient amount of photons such that leaving the band is possible. However, for the lower bands is known the existence of a gap. If the photon energy is even low that the energy gap between bands, the natural question is what happens as the wavepacket absorbs energy in the gap regime. Examples of scattering diagrams are shown in the figures 4-13, 4-14 and 4-15. There, we note clearly the manifestation of fringes that corresponds to the shifted energies consequence of the scattering. The gray dotted lines are the Floquet theoretical predictions to the position of this fringes. We construct this using the shifted energy Floquet formula:

$$E_n = E_0 + n\hbar\omega$$

And applying it in the inverse of the dispersion relation $E(k)$:

$$k_n = k(E_n) = k(E_0 + n\hbar\omega)$$

Where the n is the integer number of photons traded with the driving and E_0 is the original energy of the incident wave-packet.

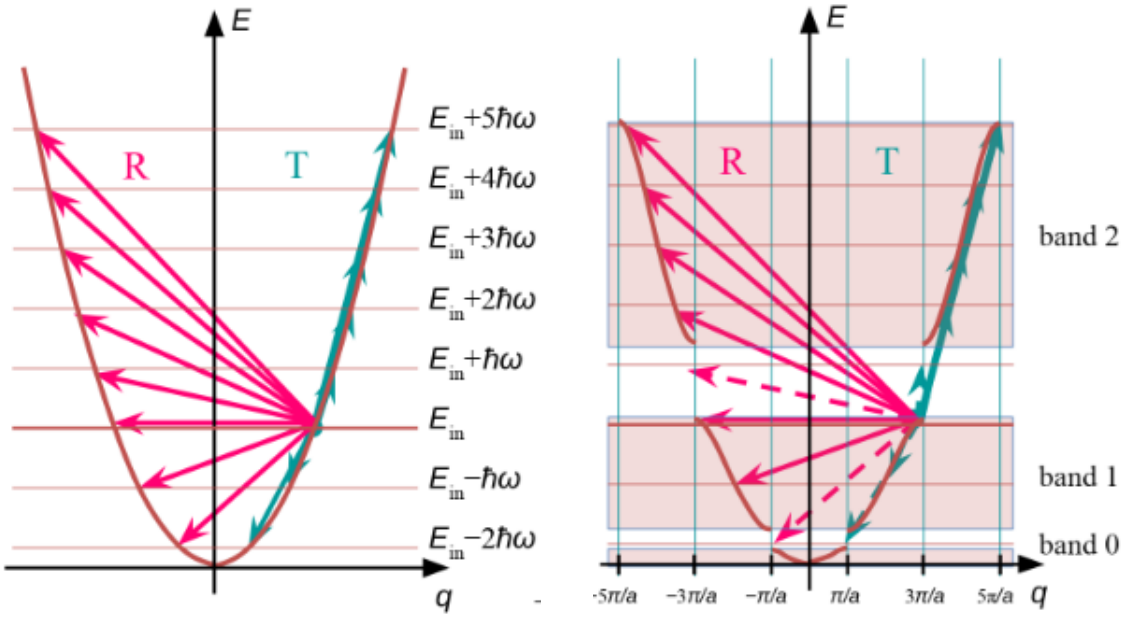

(a) Free Scattering (b) Punchet Scattering

Figura 4-12.: Floquet shifting

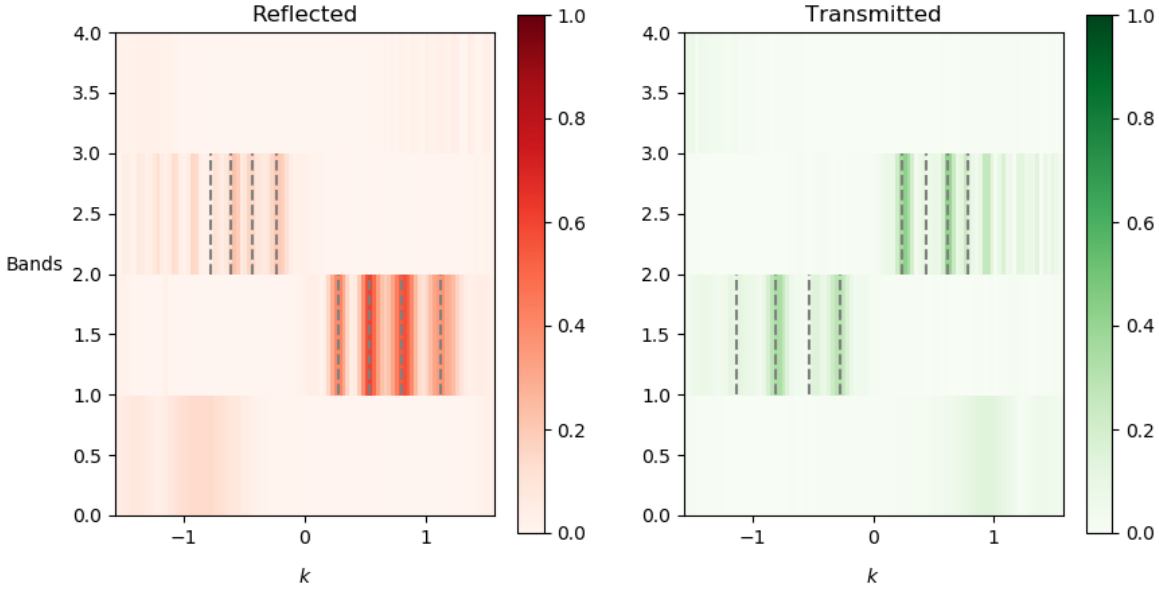

(a)

Figura 4-13.: Type I Punchet

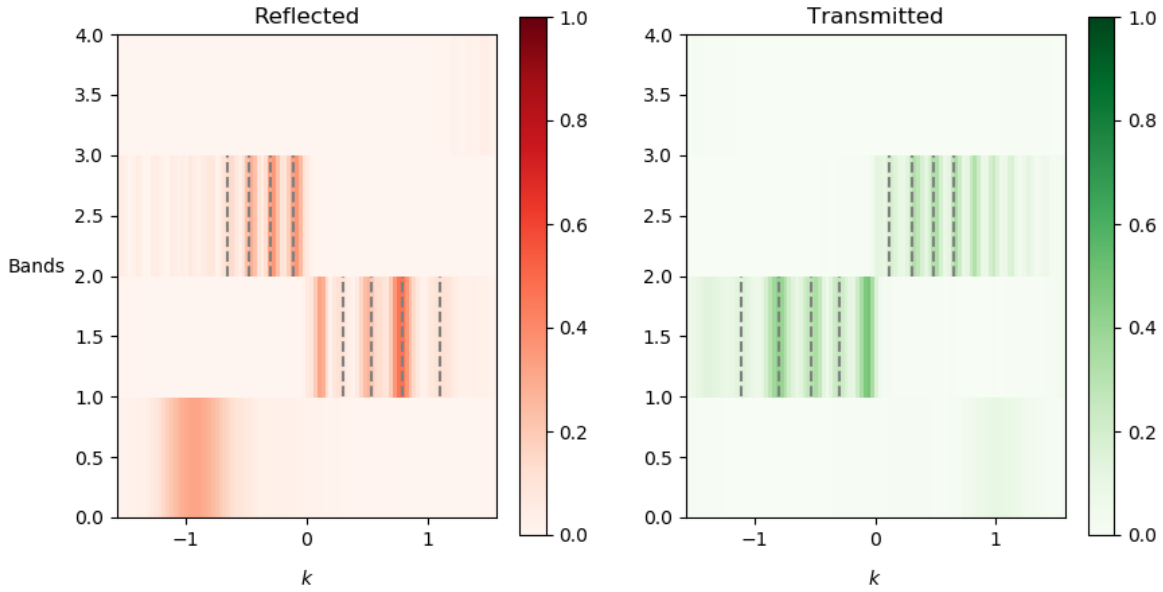

(a)

Figura 4-14.: Type II Punchet

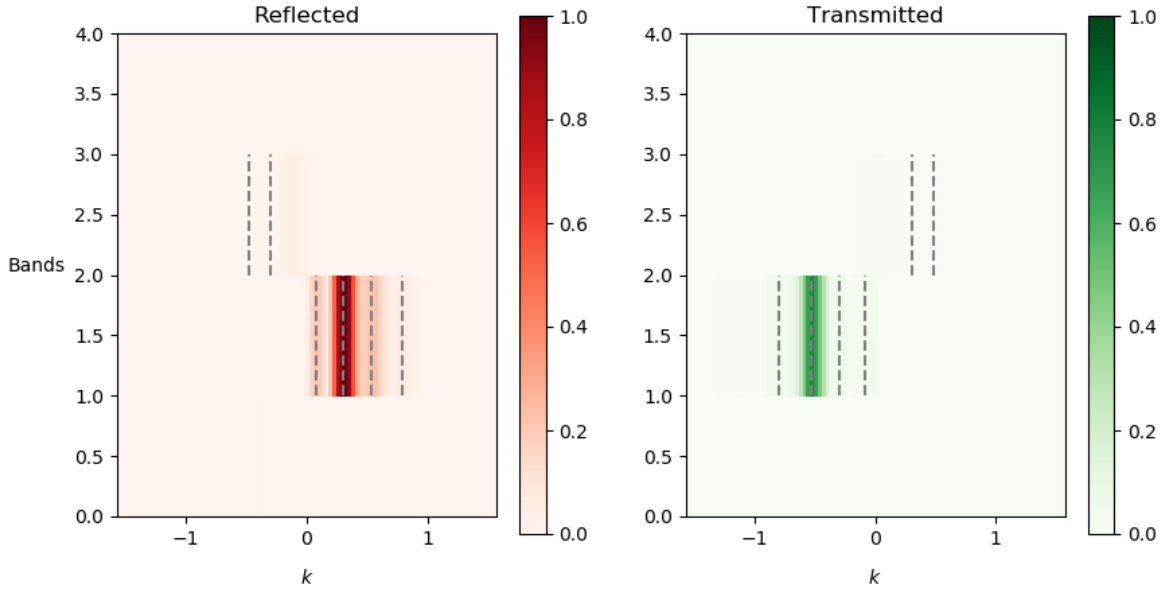

(a)

Figura 4-15.: Type III Punchet

5. Conclusions

In this thesis, we develop a theoretical approach to the manifestation of directed transport phenomena, in the framework of the hybrids between pumps and ratchets. These hybrids were only studied before in the article derived of this work [**?**]. Then, this is a new theoretical device designed by the autor and its advisor, and whose transport properties were characterized in terms of:

- Identification of complex structures typical of irregular scattering, like invariant sets induced by the driving, fractality and high oscillations in the reaction functions and fractal boundaries between the areas generated by the individual contributions to transport.
- Exemplification of the control mechanisms present in the model of punchets studied, showing how the net currents generated can be completely manipulated in terms of intensity and direction. Also manifestation of irregular nonlinear dynamics arose as in the case of the Type III punchet where it is possible to generate currents in the opposite direction of the travelling wave bounded in the scattering region.
- Proving that in the quantum version of punchets the initial Bloch states scatters to the asymptotic bands through Floquet shiftings.

Further work will consist in the quantum control of currents, studying the semi-classical regime, in order to understand the relevance of chaotic invariant sets in the generation of quantum currents and looking for connections with the topological theory that appears naturally when the driving is adiabatic.

A. Numerical Propagator

For the numerical integration of the classical and quantum dynamics, we use a fractal construction of the approximated propagator [14]. In both cases, we can write this propagator in terms of an exponential of the form:

$$G(t', t) = e^{A(t-t')}$$

Where the A is a formal operator in the general case. For classical mechanics, we have that:

$$\frac{d}{dt}\begin{pmatrix} p(t) \\ q(t) \end{pmatrix} = \begin{pmatrix} -\frac{d}{dt}V(q) \\ \frac{d}{dt}K(p) \end{pmatrix} = \begin{pmatrix} & -\hat{V} \\ \hat{K} & \end{pmatrix}\begin{pmatrix} p(t) \\ q(t) \end{pmatrix}$$

Where the previous operators $\hat{K}$ and $\hat{V}$ are formal expressions for:

$$\hat{K}p \equiv \frac{d}{dp}K(p), \qquad \hat{V}q \equiv \frac{d}{dq}V(q)$$

Then, we can write the formal *'Hamiltonian' operator*:

$$\mathcal{H} = \begin{pmatrix} & \\ \hat{K} & \end{pmatrix} + \begin{pmatrix} & -\hat{V} \\ & \end{pmatrix} = \begin{pmatrix} & -\hat{V} \\ \hat{K} & \end{pmatrix}$$

Where the first and second elements in the sum do not commute in general. Using this, we can write a formal solution for the Hamilton equations:

$$\begin{pmatrix} p(t) \\ q(t) \end{pmatrix} = e^{\mathcal{H}t}\begin{pmatrix} p(0) \\ q(0) \end{pmatrix}$$

In the quantum case, is just necessary to use the well-known expression:

$$|\phi(t)\rangle = e^{-i\hat{H}t}\,|\phi(0)\rangle$$

Then, for the classical case we have that the time-translation generator is the $\mathcal{H}$ operator and in the quantum case just the Hamiltonian operator $\hat{H}$. However, is a fact that the systems of interest in this thesis are strongly time-depedent. In this sense, the form of the propagator changes. If $A(t)$ is the time-translation, time-depedent, generator, the formal propagator is written:

$$G(t, t') = T\left[\exp\left(\alpha\int_{t'}^{t} A(t)dt\right)\right]$$

Where T is the time-ordering operator, $\alpha = 1$ for the classical case and $\alpha = -i$ in the quantum case. In order to construct an exponential approximant for this operator, we introduce the shift-time operator [26]:

$$F(t)e^{\Delta t\mathcal{T}}G(t) = F(t+\Delta t)G(t)$$

Where the operator acts on the function on the left. This operator has the form:

$$\mathcal{T} = -\alpha\frac{\partial}{\partial t}$$

Following [14], we find finally that:

$$G(t,t') = e^{\alpha(t-t')(A(t)+\mathcal{T})}$$

A.1. Fractal Exponential Decomposition

We recall that usually the time-translation generators are written as a sum of two different operators (a *kinetic* operator and a *potential* operator), that in general not commute between them. Now, we use the usual symplectic order two approximant, that is generated symmetrizing the Trotter formula for the operator $A = B + C$:

$$S_2(x) = e^{\frac{x}{2}B}e^{xC}e^{\frac{x}{2}B}$$

Where the condition $S_2(x)S_2(-x) = I$ hold. Following N. Hatano and M. Suzuki, this leads to a symmetrized fourth-order approximant:

$$S_4(x) \equiv S_2(sx)S_2((1-2s)x)S_2(sx)$$

Where the value of the real number s is determined by the condition $S_4(x)S_4(-x) = I$. This generates the following equation:

$$2s^3 + (1-2s)^3 = 0, \qquad s = \frac{1}{2-\sqrt[3]{2}}$$

Using this operator, we can generator expressions of higher-orden. This recurrence is what gives the fractal name to this method. In the time-depedent case, we have to approximate the exponential of the operator $A' = A + \mathcal{T} = B + C + \mathcal{T}$, that is, a sum of the time-translation operator plus the time-shifting operator. In this case, the order two approximant is written as:

$$S_2(x) = e^{\frac{x}{2}\mathcal{T}}e^{\frac{x}{2}B}e^{xC}e^{\frac{x}{2}B}e^{\frac{x}{2}\mathcal{T}}$$

And the higher order expression has the same structure. So, the problem reduces to compute the exponentials of each of the factors. In the classical case we just take in account that if

$\mathcal{H} = \mathcal{K} + \mathcal{V}$ as it was defined previously, then:

$$e^{\mathcal{K}\Delta t}\begin{pmatrix} p \\ q \end{pmatrix} = (I + \mathcal{K}\Delta t)\begin{pmatrix} p \\ q \end{pmatrix} = \begin{pmatrix} p \\ q + \Delta t \frac{d}{dp} K(p) \end{pmatrix}$$

$$e^{\mathcal{V}\Delta t}\begin{pmatrix} p \\ q \end{pmatrix} = (I + \mathcal{V}\Delta t)\begin{pmatrix} p \\ q \end{pmatrix} = \begin{pmatrix} p - \Delta t \frac{d}{dq} V(q) \\ q \end{pmatrix}$$

In the quantum case, we have to apply successive Fourier transforms and then multiply by the exponential factor.

B. Bloch and Floquet Theory

B.1. Bloch Wavefunctions

The Bloch theory typically applies for systems with spatially periodic Hamiltonian:

$$\hat{H}(x+L) = \hat{H}(x)$$

Then, the translation operator defined as $T(a)\,|x\rangle = |x+a\rangle$ commutes with the Hamiltonian at each period:

$$\hat{H}(x)T(L)\,|x\rangle = \hat{H}(x)\,|x+L\rangle = \hat{H}(x+L)\,|x+L\rangle = T(L)\hat{H}(x)\,|x\rangle$$

Therefore, the translation at each period operator, has an associated preserved quantity through the dynamics of the system. In other words, the Hamiltonian an T operator can be simultaneously diagonalized. This preserved quantity is the so called *quasimomentum*. Knowing the explicit form of the translation operator:

$$T(a) = e^{i\hat{p}a}$$

An eigenstate of this operator when $a = L$ is also an energy eigenstate, as we just see. Then the Hamiltonian have eigenstates of the form:

$$|\psi\rangle = e^{ikx}\,|\phi\rangle$$

Where $|\phi(x)\rangle = |\phi(x+L)\rangle$. Using this periodicity, we can expand $|\phi\rangle$ in Fourier terms. In space representation, for each k:

$$\langle x|\phi_k\rangle = \phi_k(x) = \sum_{n\in\mathbb{Z}} a_{nk} e^{2\pi i n \frac{x}{L}}$$

Then, the energy eigenstates finally has the form:

$$\langle x|\psi\rangle = \psi_k(x) = e^{ikx}\phi_n k(x)$$

Where the Fourier terms multiplied by the phase factor dependent of k configures a complete basis for the Hilbert space. Therefore, the Hamiltonian can be diagonalized in terms of this functions, where each eigenstate is characterized by the quantum numbers n and k. This corresponds to the *band number* and the *quasimomentum*, respectively.

B.2. Floquet Energy

The Floquet theory arose as a powerful tool to handle with explicitly time-periodic Hamiltonians, without any particular approximation. In this sense is very useful for systems as those shown in this thesis, where we have strong non-adiabatic periodic time-dependence. So, starting from a Hamiltonian:

$$\hat{H}(t) = \hat{H}(t+T)$$

So, in a similar approximation to the Bloch construction, we can find that the wavefunctions for this Hamiltonian can be written using the following ansatz:

$$\psi(x,t) = e^{-i\frac{\epsilon t}{\hbar}}\phi(x,t)$$

With $\phi(x,t) = \phi(x,t+T)$. The quantity ϵ is a real number called the *Floquet Energy* or *Quasienergy*. When we use this on the Schrödinger equation we arrive to the formula:

$$\left[\hat{H} - ih\frac{\partial}{\partial t}\right]\phi(x,t) = \hat{H}_F\phi(x,t) = \epsilon\phi(x,t)$$

That is basically an eigenvalue equation where we have defined the hermitic operator $\hat{H}_F$ called the Floquet Hamiltonian. One specific feature of the Floquet states is the energy shifting that occurs when we multiply the $\psi(x,t)$ states by a phase $e^{in\omega t}$. Using this and applying the modified wavefunction, we find a similar expression but with quasienergy $\epsilon' = \epsilon + n\hbar\omega$. In this sense, the quasienergy is a conserved quantity along the evolution modulo integer multiples of the energy at each driving period induced by the time-dependence [11].

Is important to note the domain of the Floquet Hamiltonian, in the sense that the Hilbert space in which the original Hamiltonian acts is not the same of the Floquet Hamiltonian. In this case we have to define de space $\mathbb{S} = \mathbb{H} \otimes \mathbb{T}$, where $\mathbb{H}$ is the original Hilbert space of the system and $\mathbb{T}$ the Hilbert space of the periodic functions. In the literature this is found as the *Sambe space*. The interior product that characterizes this Hilbert space is inherited from the factor spaces in the tensor product in the natural way. For elements $\psi, \phi \in \mathbb{S}$:

$$\langle\langle\psi|\phi\rangle\rangle = \frac{1}{T}\int_t^{t+T}\int_{-\infty}^{\infty}\psi^*(x,t')\phi(x,t')dxdt'$$

Bibliografía

[1] ALTSHULER, B. L. ; GLAZMAN, L. I.: Pumping Electrons. En: *Science* 283 (1999), Nr. 5409, p. 1864–1865. – ISSN 0036–8075

[2] BERRY, M V.: Regular and irregular semiclassical wavefunctions. En: *Journal of Physics A: Mathematical and General* 10 (1977), dec, Nr. 12, p. 2083–2091

[3] BROUWER, P. W.: Scattering approach to parametric pumping. En: *Physical Review B* 58 (1998), Oct, Nr. 16, p. R10135–R10138

[4] COHEN, Doron: Quantum pumping in closed systems, adiabatic transport, and the Kubo formula. En: *Phys. Rev. B* 68 (2003), Oct, p. 155303

[5] COHEN, Doron: Quantum pumping in closed systems, adiabatic transport, and the Kubo formula. En: *Phys. Rev. B* 68 (2003), Oct, p. 155303

[6] DUAN, Feng ; GUOJUN, Jin: *Introduction to Condensed Matter Physics*. WORLD SCIENTIFIC, 2005

[7] ESAKI, Seiji ; ISHII, Yoshiharu ; NISHIKAWA, Masatoshi ; YANAGIDA, Toshio: Cooperative actions between myosin heads bring effective functions. En: *Biosystems* 88 (2007), Apr, Nr. 3, p. 293–300

[8] FOA TORRES, L.E.F. ; CUNIBERTI, G.: AC transport in carbon-based devices: challenges and perspectives. En: *Comptes Rendus Physique* 10 (2009), May, Nr. 4, p. 297–304

[9] GERWINSKI, P. ; ŠEBA, P.: Quantum resonances due to classical stability islands. En: *Physical Review E* 50 (1994), Nov, Nr. 5, p. 3615–3622

[10] GORRE-TALINI, L. ; JEANJEAN, S. ; SILBERZAN, P.: Sorting of Brownian particles by the pulsed application of an asymmetric potential. En: *Phys. Rev. E* 56 (1997), Aug, p. 2025–2034

[11] GRIFONI, Milena ; HÄNGGI, Peter: Driven quantum tunneling. En: *Physics Reports* 304 (1998), Oct, Nr. 5–6, p. 229–354

[12] GUDDE, J. ; ROHLEDER, M. ; MEIER, T. ; KOCH, S. W. ; HOFER, U.: Time-Resolved Investigation of Coherently Controlled Electric Currents at a Metal Surface. En: *Science* 318 (2007), Nov, Nr. 5854, p. 1287–1291

[13] HACHÉ, A. ; KOSTOULAS, Y. ; ATANASOV, R. ; HUGHES, J. L. P. ; SIPE, J. E. ; VAN DRIEL, H. M.: Observation of Coherently Controlled Photocurrent in Unbiased, Bulk GaAs. En: *Physical Review Letters* 78 (1997), Jan, Nr. 2, p. 306–309

[14] In: HATANO, Naomichi ; SUZUKI, Masuo: *Finding Exponential Product Formulas of Higher Orders*. Berlin, Heidelberg : Springer Berlin Heidelberg, 2005, p. 37–68. – ISBN 978–3–540–31515–5

[15] HENSELER, Michael ; DITTRICH, Thomas ; RICHTER, Klaus: Classical and quantum periodically driven scattering in one dimension. En: *Physical Review E* 64 (2001), Sep, Nr. 4

[16] KOUMURA, Nagatoshi ; ZIJLSTRA, Robert W. J. ; VAN DELDEN, Richard A. ; HARADA, Nobuyuki ; FERINGA, Ben L.: Light-driven monodirectional molecular rotor. En: *Nature* 401 (1999), Sep, Nr. 6749, p. 152–155

[17] LAU, Bryan ; KEDEM, Ofer ; SCHWABACHER, James ; KWASNIESKI, Daniel ; WEISS, Emily A.: An introduction to ratchets in chemistry and biology. En: *Materials Horizons* 4 (2017), Nr. 3, p. 310–318. – ISSN 2051–6347

[18] MATTHIAS, Sven ; MÜLLER, Frank: Asymmetric pores in a silicon membrane acting as massively parallel brownian ratchets. En: *Nature* 424 (2003), Jul, Nr. 6944, p. 53–57

[19] MIKHNENKO, Oleksandr V. ; COLLINS, Samuel D. ; NGUYEN, Thuc-Quyen: Rectifying Electrical Noise with an Ionic-Organic Ratchet. En: *Advanced Materials* 27 (2015), Feb, Nr. 12, p. 2007–2012

[20] MURILLO, Gustavo: *Control de las propiedades electrónicas en semiconductores cuasi-unidimensionales por medio de campos AC: aproximación de Floquet*. Cali, Colombia, Universidad del Valle, Tesis de Grado, 2013

[21] VAN OUDENAARDEN, A.: Brownian Ratchets: Molecular Separations in Lipid Bilayers Supported on Patterned Arrays. En: *Science* 285 (1999), Aug, Nr. 5430, p. 1046–1048

[22] POTHIER, H. ; LAFARGE, P. ; URBINA, C. ; ESTEVE, D. ; DEVORET, M. H.: Single-Electron Pump Based on Charging Effects. En: *EPL (Europhysics Letters)* 17 (1992), Nr. 3, p. 249

[23] ROUSSELET, Juliette ; SALOME, Laurence ; AJDARI, Armand ; PROSTT, Jacques: Directional motion of brownian particles induced by a periodic asymmetric potential. En: *Nature* 370 (1994), Aug, Nr. 6489, p. 446–447

[24] SCHANZ, Holger ; OTTO, Marc-Felix ; KETZMERICK, Roland ; DITTRICH, Thomas: Classical and Quantum Hamiltonian Ratchets. En: *Phys. Rev. Lett.* 87 (2001), Jul, p. 070601

[25] STOOF, T. H. ; NAZAROV, Yu. V.: Time-dependent resonant tunneling via two discrete states. En: *Phys. Rev. B* 53 (1996), Jan, p. 1050–1053

[26] SUZUKI, Masuo: General Decomposition Theory of Ordered Exponentials. En: *Proceedings of the Japan Academy, Series B* 69 (1993), Nr. 7, p. 161–166

[27] TENNIE, Claudio ; CALL, Josep ; TOMASELLO, Michael: Ratcheting up the ratchet: on the evolution of cumulative culture. En: *Philosophical Transactions of the Royal Society B: Biological Sciences* 364 (2009), Aug, Nr. 1528, p. 2405–2415

[28] THOULESS, D. J.: Quantization of particle transport. En: *Phys. Rev. B* 27 (1983), May, p. 6083–6087

[29] TIERNO, Pietro ; REIMANN, Peter ; JOHANSEN, Tom H. ; SAGUÉS, Francesc: Giant Transversal Particle Diffusion in a Longitudinal Magnetic Ratchet. En: *Physical Review Letters* 105 (2010), Dec, Nr. 23